PERGAMON

Journal of Structural Geology 23 (2001) 1677–1699

JOURNAL OF STRUCTURAL GEOLOGY

www.elsevier.com/locate/jstrugeo

Thrust-related, diapiric, and extensional doming in a frontal orogenic wedge: example of the Montagne Noire, Southern French Hercynian Belt

Jean-Claude Soula[a,*], Pierre Debat[b], Stéphane Brusset[a], Gilbert Bessière[a], Frédéric Christophoul[a], Joachim Déramond[a]

[a]*Laboratoire de Dynamique des bassins sédimentaires, Université Paul Sabatier, 38, rue des Trente-Six-Ponts, 31400 Toulouse, France*
[b]*Laboratoire Transfert de Matière, UMR 5563, Université Paul Sabatier, 38, rue des Trente-Six-Ponts, 31400 Toulouse, France*

Received 12 January 2000; revised 20 January 2001; accepted 7 February 2001

Abstract

The Montagne Noire, which is situated at the toe of the orogenic wedge of the French Massif Central South European Variscides, appears to be a well-suited area for studying the origin and evolution of middle to upper crustal domes adjacent to foreland basins. The data reported in the present paper show that the Montagne Noire dome is a particular type of basement-involved frontal culmination in an orogenic wedge and foreland basin system. This frontal culmination is characterized by a syn-contractional HT decompression recorded by clockwise PTt paths and widespread strata overturning in thrust and fold structures, which controlled the sedimentation in the adjacent foreland basin. These unusual characteristics are interpreted to be a result of the succession of thrusting, diapirism and extensional collapse. Antiformal stacking of syn-metamorphic thrust sheets controlled the first stages of the foreland basin development. Diapirism was essentially responsible for the HT decompression and widespread strata overturning. Extensional doming was a result of late- to post-metamorphic collapse acting on the pre-existing high-amplitude dome. Diapirism and associated isothermal decompression metamorphism, which constitute the essential difference between the Montagne Noire and 'ordinary' frontal ridges in orogenic wedges, were probably enhanced by a local partial melting of the upper to middle crust. It is suggested that the occurrence of these phenomena in front of an orogenic wedge was related to local over-thickening due to the superposition of an upper crustal antiformal stack on top of a lower crustal ramp anticline.

Keywords: Montagne Noire; Orogenic wedge; Foreland basin; Metamorphism; Diapirism

1. Introduction

Domes are frequent in mountain belts and may have formed in various tectonic settings and at various times during the tectonic history. Several mechanisms have been proposed to explain doming, including large-scale buckling (e.g. Ramsay 1967, p. 384; Snowden and Bickle, 1976), antiformal stacking and other thrust-related processes (Perez-Estáun et al., 1991; McClay, 1992a,b; Burkhard and Sommaruga, 1998; DeCelles et al., 1998), post-contractional extension (e.g. Davis and Coney, 1979; Wernicke, 1981; Wernicke and Burchfiel, 1982; Allmendinger et al., 1983; Ménard and Molnar, 1988; Marshak and Alkmin, 1989; Echtler and Malavieille, 1990; Brun et al., 1994; Vissers et al., 1995; Holm and Lux, 1996; Schneider et al., 1996; Marshak et al., 1997), syn-contractional gravitational collapse (and/or denudation) (e.g. Philippot, 1990; Seward and Mancktelow, 1994; Steck and Hunziker, 1994; Aerden, 1998; Stüwe and Barr, 1998; Aerden and Malavielle 1999) and diapirism (Soula et al., 1986; Delor et al., 1991; Audren and Triboulet, 1993; Hippertt, 1994; Bouhallier et al., 1995; Choukroune et al., 1995; Shackleton, 1995; Talbot and Koyi, 1995; Warren and Ellis, 1996; Dirks et al., 1997; Chardon et al., 1998; Calvert et al., 1999; De Bremond d'Ars et al., 1999; Hippertt and Davis, 2000).

Domes are observed at various places in a mountain belt. In the external parts of orogenic wedges, domes are most often antiformal stacks. These structures, even basement involved, are, in general, free of metamorphism. This is the case, for example, in the External Massifs of the western Alps (e.g. Burkhard and Sommaruga, 1998) or the Ramgahr–Dadeldhura–MBT thrusts zone in the Himalayas (DeCelles et al., 1998) or the Variscides of northwest Spain (Perez-Estáun et al., 1991).

The Montagne Noire constitutes the more external ridge of the South European Variscides (French Massif Central

* Corresponding author.
E-mail address: geostruc@cict.fr (J.-C. Soula).

0191-8141/01/$ - see front matter
PII: S0191-8141(01)00021-9

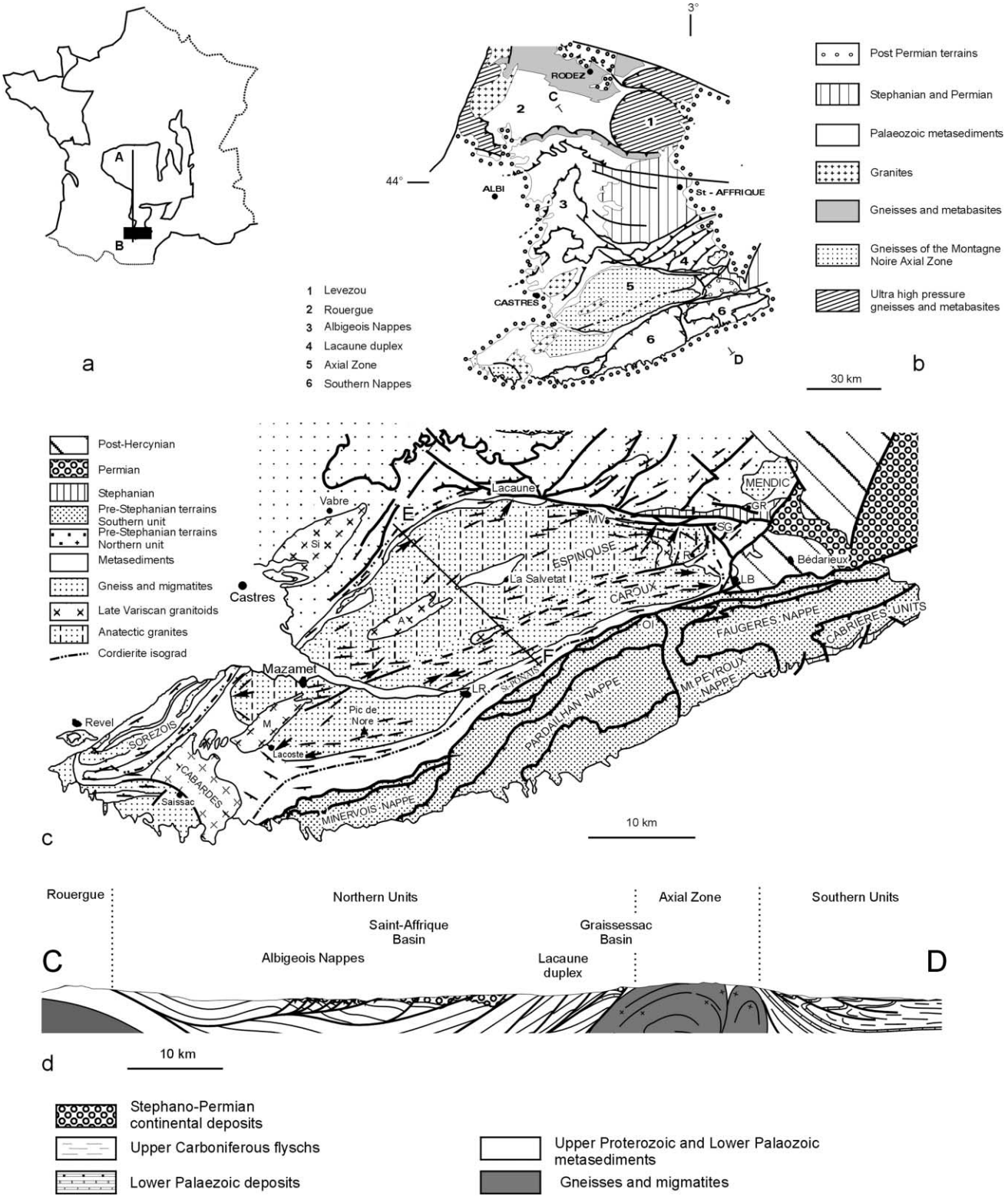

Fig. 1. (a) Location of the study area. Variscan domain is delineated. Location of the cross-section in Fig. 2 is indicated (AB). (b) Map of the south-western French Massif Central (modified after Guérangé-Lozes and Burg, 1990). Location of cross-section in (c) (below) and in Fig. 9 is indicated (CD). (c) Geological map of the Montagne Noire. Location of the cross-section in Fig. 7 is indicated (EF). A: Anglès; GR: Graissessac; LB: Lamalou-les-bains; LR: Labastide–Rouairoux; MV: Murat-sur-Vèbre; Ol: Olargue; R: Rosis; SG: Saint Gervais; SI: Sidobre. (d) Geological profile after Guérangé-Lozes (1987 and unpublished), Guérangé-Lozes and Burg (1990), Donnot and Guérangé (1978), Burg et al. (1989), Arthaud (1970), Echtler and Malavieille (1990), Beaud (1985), Ferret (1983), Ourzik (1993) and Matte et al. (1998), completed by personal observations of the authors.

domain) (Engel and Franke, 1983; Matte, 1991). Just adjacent to the foredeep, it is similar to the 'triangle zones' of DeCelles and Giles (1996), but doming is associated with high temperature–medium-to-low pressure metamorphism. The question thus arises of the mechanism of development of syn-metamorphic domes in such an external tectonic position.

The Montagne Noire appears as a favorable area for answering the question since it has long been proposed as a model of dome developed by practically all the mechanisms recalled above.

The present study is based on the construction of balanced cross-sections and on a new structural analysis of the dome-envelope contact zone, including strain estimates, shear criteria, timing relationship between mylonitic structures and metamorphism. A new model of development of the fold-and-thrust structures in the foreland basin during turbiditic sedimentation is then proposed. This study also integrates a synthesis of the data presently available on metamorphism, microstructures, metamorphism-tectonics-sedimentation relationships, radiometric and palaeontological dating.

2. Characteristics of the Montagne Noire and surroundings

2.1. Situation and overall structure of the Montagne Noire

The Montagne Noire is the most external ridge of the French Massif Central, which is generally considered as the south-vergent orogenic wedge of the South European Variscides, and is directly adjacent to the southern foreland basin (Engel and Franke, 1983; Franke and Engel, 1986; Matte, 1991) (Figs. 1 and 2). The Massif Central is characterized by a high temperature–low-to-medium pressure metamorphism and is overriden by ultra-high pressure (UHP) granulites and eclogites which are likely to represent remnants of a subducted continental crust with attached oceanic crust slices (Bodinier et al., 1986; Burg et al., 1989). The southernmost outcrops of the UHP granulites and eclogites are observed in the Levezou and Vibal domes presently situated 60 km to the N of the Montagne Noire (Fig. 1b). According to Matte (1991, fig. 5C), these rocks have been transported southward by more than 200 km over the mid-crustal rocks of the orogenic wedge (Figs. 1 and 2).

The Montagne Noire ridge (Fig. 1b and c) is broadly constituted of three ENE–WSW trending structural units (Gèze, 1949): (1) the northern units composed of greenschist facies lower Paleozoic series involved in south-eastward-vergent thrust sheets (Donnot and Guérangé, 1978; Guérangé-Lozes, 1987; Guérangé-Lozes and Burg, 1990); (2) the Axial Zone forms a ENE–WSW trending elongate dome essentially composed of migmatized orthogneisses known as the Agout Dome (Gèze, 1949; Schuiling, 1960) enveloped by metasediments usually defined as the 'schistes X' (Gèze, 1949) and locally intruded by late-Hercynian granodiorites (Fig. 1b and c); and (3) the southern units characterized by the stacking into the Visean foreland basin of southerly transported thrust sheets in which are involved low grade to non-metamorphic Cambrian to Lower Carboniferous terrains (Arthaud, 1970; Engel et al., 1980–1981;).

The Agout Dome is divided into two N 70E trending second order domes, the Espinouse and Caroux–Pic de Nore domes (Beaud, 1985; Faure and Cottereau, 1988; Ourzik, 1993), which are separated by a steep-dipping fault (Fig. 1c and d). The migmatized gneisses are predominantly granitic orthogneisses. Metasedimentary septa such as metapelites, metaquartzites and marbles are found in the Espinouse sub-dome. Metabasic septa are also observed. Some of them, found as several metre thick enclaves within anatectic granitoids, have been interpreted as derived from 'relatively low pressure' eclogites with initial PT conditions of 700–800°C and 9 ± 2kb (Demange, 1982, 1985, 1998).

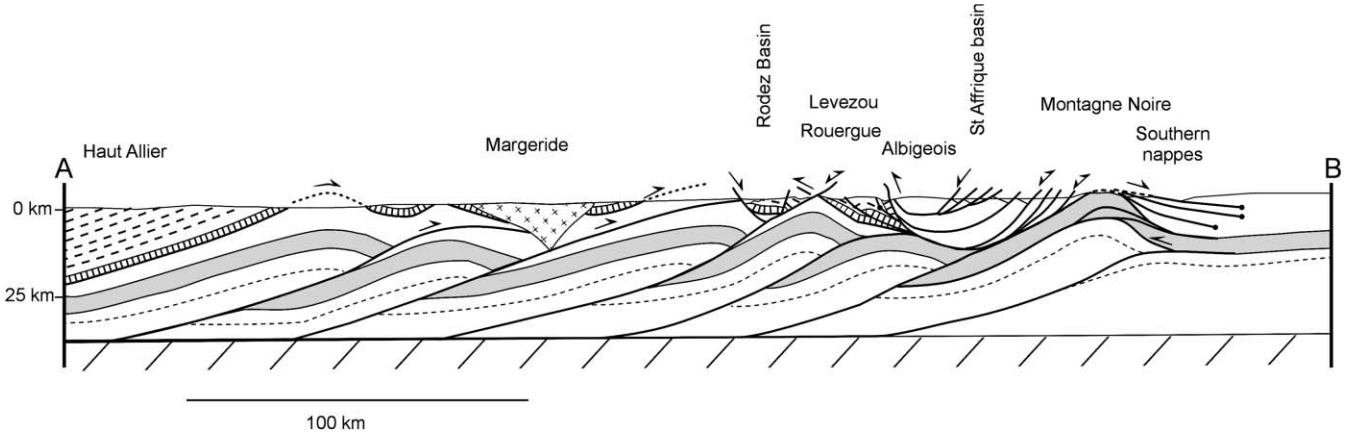

Fig. 2. Balanced cross-section through the French Massif Central orogenic wedge. Northern part after Matte (1991) modified because of balance requirements. Southern part incorporates section shown in Fig. 10e.

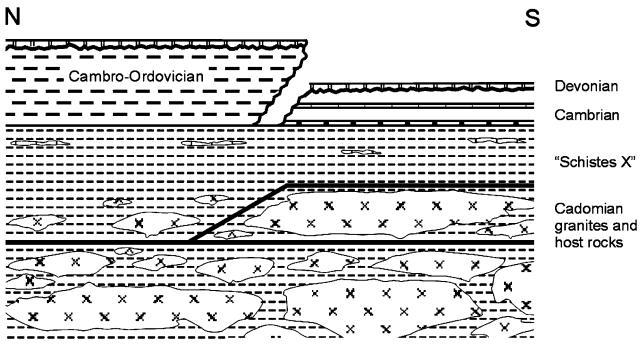

Fig. 3. Schematic representation of the Lower Paleozoic and Upper Neoproterozoic series in the Montagne Noire area (not to scale). The basal part of this series shows numerous tabular granitoid intrusions. Flats and ramps probably formed between the main granitoid sheets. To the north, the Cambro–Ordovician deposits are thick deep-marine terrigenous basinal deposits; to the south, the Cambro–Ordovician deposits are shelf deposits. The Lowermost Cambrian sandstones and the Upper Cambrian limestones shown in the top-right part of the sketch are used as marker beds in the balanced cross-sections (Fig. 10).

2.2. Initial configuration

The stratigraphic pile of the Montagne Noire is constituted of Neoproterozoic and Paleozoic rocks. According to Bard (1978a) and Bard and Loueyit (1978), the Proterozoic rocks were originally a thick series of detrital shales with occasional volcanic and carbonate interbeds. The uppermost part of this series has been dated of 545 ± 15 Ma on single zircons from metadacites interlayers (step-wise Pb evaporation method, Lescuyer and Cocherie, 1992). The lower part of this series was intruded by large and almost contiguous granitic sheets (Fig. 4) then deformed to constitute the orthogneisses (Debat et al., 1971; Debat, 1974). The emplacement of these granitic sheets has been dated as 513 ± 13 Ma on zircons from the orthogneisses (Ducrot et al., 1979) and has been ascribed to the 'post-Cadomian' extension (Reille, 1978; Bard, 1979).

The lower part of the Paleozoic series differs markedly from north to south (Figs. 3 and 10a). To the north (Albigeois), only Cambro–Ordovician deposits are exposed. They are essentially thick (>5 km) deep-marine terrigenous basinal deposits (Courjault-Radé, 1985; Guérangé-Lozes, 1987; Guérangé-Lozes and Burg, 1990). To the south, the Cambro–Ordovician, Devonian and middle Carboniferous are represented by shelf deposits (Arthaud, 1970). It can be reasonably assumed that during early to middle Paleozoic, the northern sediments were deposited in an extensional basin resulting from crustal and probably lithospheric thinning (Matte, 1991) while the southern platform was covered by shallow-marine deposits (Figs. 3 and 10a).

2.3. Succession of the deformational events in the Axial Zone

The succession of the three major microstructural events in the Montagne Noire meets now with general agreement (see references in, e.g. Debat and Vidal (1981), Cassard et al. (1993), Demange (1996, 1998), Aerden (1998) and Matte et al. (1998)). The first deformation, D1, is characterized by a strong preferred orientation of metamorphic minerals and by flattened isoclinal microfolds. Microfold hinges deformed by D1 have been interpreted by some authors as relics of either recumbent (e.g. Demange, 1998; Matte et al., 1998) or upright folds (Aerden, 1998) but are more probably a result of progressive deformation (Ourzik, 1993). As pointed out by Faure and Cottereau (1988) or Matte et al. (1998), the existence of large syn-D1 recumbent folds must be seriously questioned. However, the presence in the eastern Axial Zone of some hundred metre-spaced thrusts and associated ductile shear zones domed together with S1 (Bard, 1978b), suggests syn-D1 imbricate thrusting. The second deformation, D2, is represented by upright folds F2 associated with a crenulation cleavage S2. F2 folds are clearly identified in the central part of the gneiss dome and in the envelope outside the contact with the gneisses. F2 fold axes and L2 stretching lineations are sub-parallel to the long axis of the dome. These fold axes and stretching lineations are sub-horizontal in the north-western and south-eastern flanks, and dip to the NE in the north-eastern and to the SW in the south-western extremities of the dome. The third deformation, D3, is responsible for open to tight folds F3 with wavelengths of about a few centimetres to several metres associated with a crenulation cleavage S3 (Beaud, 1985; Aerden, 1998). F3 folds locally pass into mesoscopic ductile shear zones. As already shown by Beaud (1985), S3 is subhorizontal and sub-parallel to S1 in the central part of the dome and become more steeply inclined towards the periphery (50–70° average dip to the NW and SE; 20–40° average dip to the NE and SW). F3 fold axes are sub-parallel to the contours of the dome (Faure and Cottereau, 1988; Ourzik, 1993) whereas stretching lineations L3 are sub-parallel to the long axis of the dome and to the L2 stretching lineations (Faure and Cottereau, 1988; Aerden, 1998).

Moderately to gently-dipping late shear zones D4 are observed in the south-eastern end of the dome. These shear zones indicate normal-sense displacements but should not be confused with the more steeply inclined D3 shear zones. Late upright folds D5 and/or vertical low temperature ductile shear zones are observed near the north-eastern boundary fault and have been interpreted as a result of either wrench tectonics with a minor component of normal faulting (Arthaud, 1970; Demange, 1993; Matte et al., 1998) or ductile-brittle normal faulting (Echtler and Malavieille, 1990; Cogné et al., 1993; Brun and Van Den Driessche, 1994). However, the component of transcurrent shearing inferred from microtectonic markers did not give rise to large map-scale strike-slip displacements, whereas large extensions have been inferred from the study of the Stephano–Permian basins (≧6 km, Legrand, 1990; >15 km, Burg et al., 1994). Near the south-eastern

boundary, post-D3 upright folds (D5?) have been related to a 'probably dextral shear zone' (Aerden, 1998).

2.4. Finite strain in the Axial Zone

In the gneissic core, the strain ellipsoids are oblate (flattening type) with the *X* axis trending sub-parallel to the long axis of the dome (Faure and Cottereau, 1988; Ourzik, 1993; Brunel and Lansigu, 1997). The *X*/*Y* ratio is close to one in the central and western parts of the dome (Debat et al., 1975; Faure and Cottereau, 1988; Ourzik, 1993), and close to 2.5 in the north-eastern extremity (Brunel and Lansigu, 1997). In the major part of the dome, the deformation resulted essentially from coaxial strain. Structures indicative of non-coxial strain are observed near the contact between the gneissic core and the envelope (Beaud, 1985; Faure and Cottereau, 1988; Ourzik, 1993). In the envelope outside of the contact, the deformation associated with F2 and F3 folds indicate flattening-type strain ellipsoids with the *Z* axis sub-perpendicular to the contours of the dome. The *X* axis is sub-parallel to these contours. It is horizontal in the north-western and south-eastern sides and dips outward in the north-eastern and south-western extremities.

2.5. Metamorphism

The metamorphism of the envelope has been essentially defined in the eastern side of the dome (Fig. 4). Two successive metamorphic stages may be recognized. Stage 1 metamorphism was prograde with the succession of biotite, staurolite, kyanite, and prismatic sillimanite zones. Stage 2 metamorphism is represented by well-defined isograds with the succession of biotite II, cordierite, andalusite, and fibrolitic sillimanite zones. Stage 1 and Stage 2 minerals are all aligned with S1 and the succession of the mineral assemblages is interpreted here as a continuous process occurring during progressing strain (Ourzik, 1993). Melting is nowhere present in the envelope. Stage 3 metamorphism is marked by biotite flakes and occasional fibrolitic sillimanite needles aligned with S3 near the contact with the gneisses.

The metamorphism in the migmatized gneisses reflects three stages in the evolution of P/T conditions with time. Stage 1 is characterized by the assemblage Bt + Sill + Qtz + Gt + Cd. Cordierite 1 essentially developed in the paleosomes of the metasedimentary septa (Mazamet and La Salvetat areas). Stage 2 is characterized by the development of retrogressive assemblages such as cordierite 2 rimming garnet. This textural feature is indicative of an early higher pressure assemblage (garnet + sillimanite) overprinted by a lower pressure assemblage containing cordierite as a stable phase. As in the envelope, Stage 1 and Stage 2 minerals are aligned with S1. Stage 3 metamorphism is recorded by biotite-fibrolitic sillimanite assemblages aligned with S3, which formed, in particular, the 'sillimanite nodules' of the eastern termination of the Espinouse dome (Bogdanoff, 1969; Beaud, 1985; Brunel and Lansigu, 1997). The close relationship between Stage 3 and Stage 2 minerals in both core and envelope strongly suggests a progressive evolution in the metamorphic conditions from D1 to D3. Low temperature metamorphism is associated with the late shear zones.

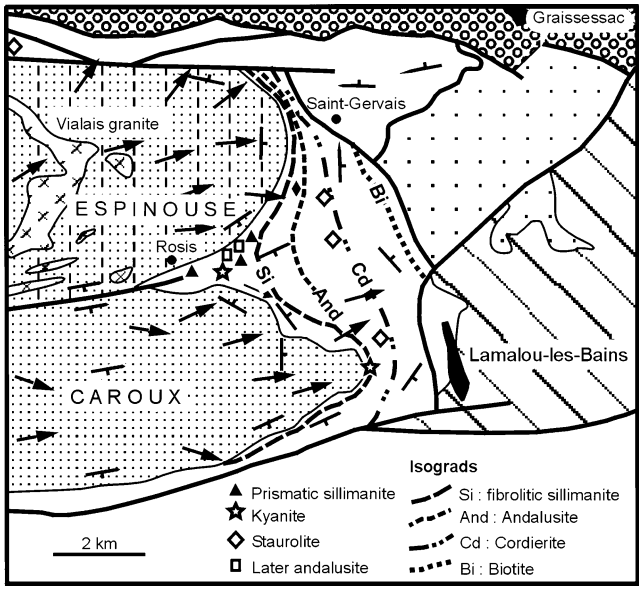

Fig. 4. Geological and structural sketch of the eastern termination of the Agout Dome showing Stage 2 metamorphic isograds and the occurrence of Stage 1 characteristic minerals. Also shown are the dips of the major regional foliation S1 and the stretching lineations (arrows). Same ornament as Fig. 1.

2.6. Migmatization

As pointed out above, the migmatites of the Axial Zone derive almost entirely from granitic orthogneisses. Although melt proportions may vary from ~5% to more than 40% at outcrop scale, it is quite impossible to distinguish and separate by mapping metatexites and diatexites. In fact, actual diatexites, i.e. highly granitized rocks where "molten and unmolten portions can no longer be distinguished" and showing 'turbulent' structures (Mehnert, 1968, p. 253) are rather infrequent. Two types of leucosomes can be distinguished, which differ by their composition and their relationship with the successive deformational events:

Type 1 leucosomes are composed of quartz (~40%), plagioclase (An 20–30) (~40%), K-feldspar (Ab ~10) (~10%), biotite (≤5%), secondary muscovite (≤2.5%), and accessories. Cordierite is occasionally observed in the thickest veins. Grain size varies from 0.5 mm to 1 cm as a function of the thickness of the veins. Two sub-types of veins can be distinguished.

Type 1a veins are oriented and boudinaged parallel to the S1 foliation. In the less migmatized parts of the augen gneisses, these veins have thicknesses ranging from a few millimetres to some centimetres and are widely-spaced.

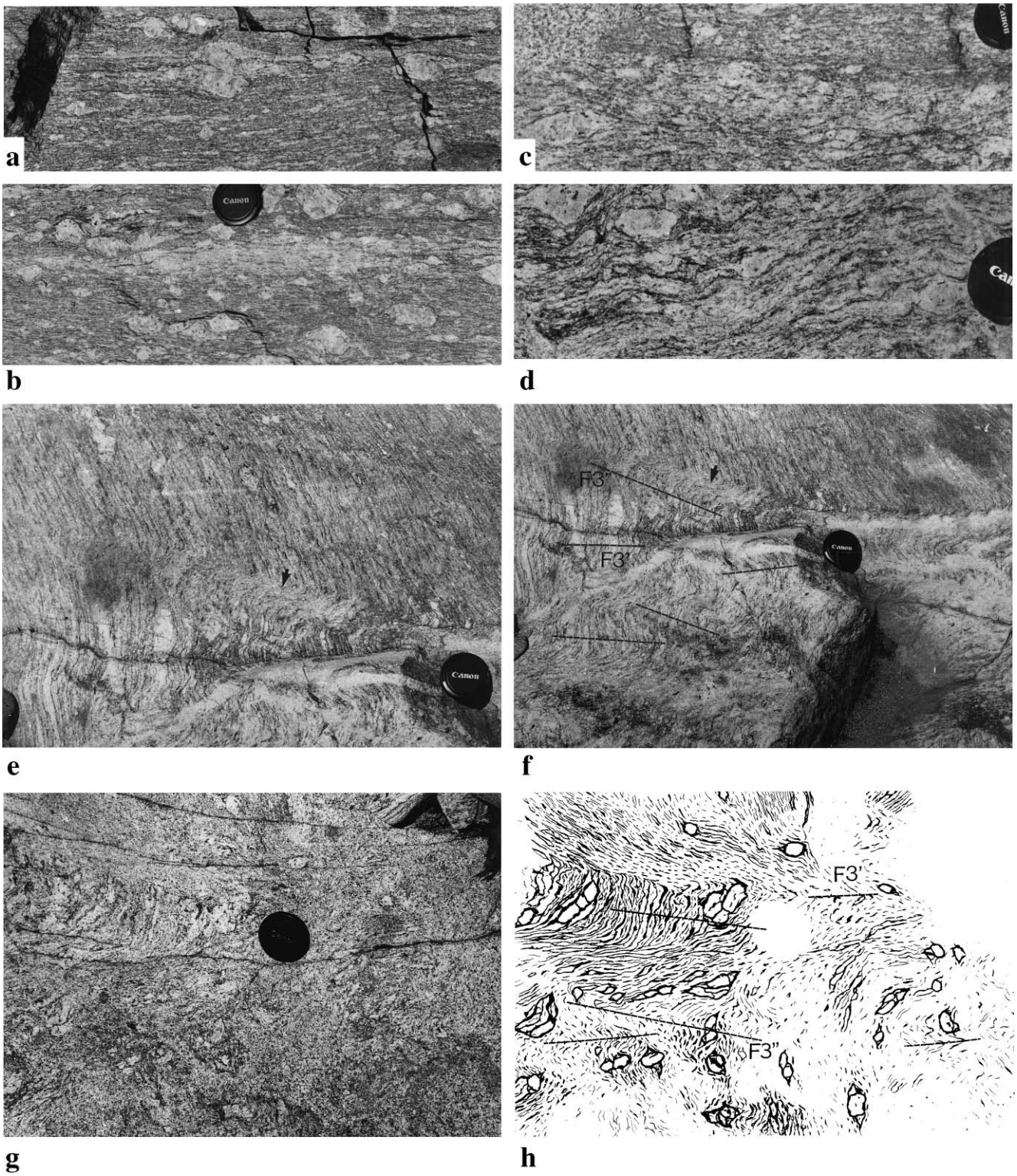

K-feldspar megacrysts, representing relics of the augen of the gneisses and protected from melting by biotite rims, are frequent (Fig. 5). The associated melanosome is represented by a thin biotite layer and/or a narrow band depleted in quartz and plagioclase (Fig. 5a–d). Locally, the leucosome only appears on both tips of K-feldspar augen as pressure-shadows that may grade into more or less continuous veins (Fig. 5a and b). With increasing migmatization, the spacing of the veins decreases, the melanosome increases in thickness at the expense of the paleosome and the rock acquires a stromatic structure (Mehnert, 1968; Brown, 1979) (Fig. 5d and e). Type 1a veins and associated melanosomes could be interpreted as differentiation structures resulting from syntectonic (syn-D1) melt segregation at local scale (see

Mehnert, 1968; Robin, 1979; Brown and Solar, 1998, amongst others).

Type 1b veins are similar to Type 1a veins, except that they are oblique to the S1 foliation. Depending on their orientation with respect to S1, these veins are either boudinaged or folded with S1 as axial plane. Type 1 veins are all present within the dome and may reach about 40 vol% without loss of the host rock's coherency, as also observed in other migmatite areas (e.g. Vanderhaeghe, 1999, p. 42). They are in many respects similar to the "diffuse concordant and discordant granitic veins" described by Vanderhaeghe (1999, figs. 5 and 6) but no undeformed veins of this type have been observed here.

*Type 2 leucosomes*appear as discordant veins, dikes or patches with sharp or diffuse contacts, often at high angles to the regional foliation. The composition of the veins is that of an aluminous granite with quartz (30–35%), K-feldspar (25–28%), plagioclase (An 10–15) (25–28%), primary muscovite (1–10%) and biotite (2–5%). The widest bodies may contain, in addition, noticeable amounts of cordierite, garnet, and more rarely andalusite (1.5–3 vol%, Schuiling, 1960; Aerden and Malavielle, 1999; Ourzik, 1993). This composition contrasts with that of Type 1 veins, which contain a more calcic plagioclase, a small amount of K-feldspar and no primary muscovite, and indicates that the temperature of crystallization of Type 2 leucosomes was lower. Also in contrast with Type 1 veins, the texture of Type 2 leucosomes is most often granophyric with a regular grain size of ~1–3 mm. Type 2 veins range in thickness from ~1 to ~10 cm and their length does not exceed a few metres in any direction. Type 2 dikes have thicknesses ranging from about 10 cm to several metres and lengths from a few metres to several tens of metres or more in the case of the wider ones. Late pegmatites are frequently related to Type 2 leucogranitic bodies. Where these leucogranitic bodies are most abundant, their association defines heterogeneous massifs with irregular and diffuse boundaries containing large fractions of host-rock. As pointed out above, they neither penetrate the metasedimentary envelope nor form large sheets localized along the core-envelope interface, which contrasts with other migmatite-cored domes (e.g. Brown and Solar, 1998, 1999; Vanderhaeghe, 1999).

Type 2 leucosomes intrude or include D2 and D3 structures. The narrow veins are more or less parallel to S2 or S3 but did not necessarily intrude along the axial plane of the folds. Small-scale diffuse patches may have occasionally formed along small-scale shear zones formed on the limbs of the folds at low angles to the axial plane (Fig. 5e and f), thus suggesting that shearing enhanced local melting during D3. Sub-horizontal dikes more or less aligned with S3 are not rare (Fig. 6c) but the large dikes are most frequently subvertical and perpendicular to S3, which strongly suggest that they were emplaced within syn-D3 extension fractures. Moreover, the direction of the vertical dikes is consistent with the strain ellipsoids determined using microstructural markers: in the eastern end of the dome where the *X* axis of the strain ellipsoid is ENE–WSW, the Vialais Massif is close to NNW–SSE (Beaud 1985; Brunel and Lansigu, 1997; Matte et al., 1998) whereas, in the north-central and western parts of this dome where the *X*/*Y* ratio is close to one, the direction of the dikes varies between E–W and N–S (Debat, unpublished). Other lines of evidence favor late-D2 to syn-D3 emplacement:

1. Several of the leucogranitic bodies aligned with S3 are locally deformed by D3 (e.g. the Mazamet granite (Debat, 1974; Ourzik, 1993) or the Vialais granite (Matte et al., 1998)).
2. The syn-D3 sillimanite nodules of the eastern termination of the Espinouse Dome are related to the emplacement of the Vialais granite (Beaud, 1985; Brunel and Lansigu, 1997).
3. Late pegmatites related to the leucogranites may intrude along the axial plane of F3 fold and are boudinaged parallel to S3 (Latouche, 1968, fig. 9; Aerden, 1998).

Fig. 5. (a) Type 1 leucosomes forming as elongate pressure shadows at the tips of K-feldspar augen protected from melting by a biotite rim. Note the thin but numerous discontinuous leucosomatic layers initiated by small feldspar augen. These layers are bounded by biotite films. (b) Type 1 leucosome. Thicker but discontinuous layer forming from coalescing biotite-bound thin layers. Biotite-rimmed K-feldspar augen are still visible within the layer. (c) Type 1 leucosome. More advanced stage of layering development owing to differentiation and melt segregation. The leucosomatic layer is bounded by two dark ('melanosometic') zones representing the paleosome impoverished in quartz and feldspars. Ghosts of biotite-rimmed K-feldspar augen are still visible both in leucosome and melanosome. On the top-left corner of the photograph, a Type 2 leucosome patch crosscut the layering with no textural continuity. (d) Type 1 leucosome. Progressive development of layering. The original augen structure is practically unaltered in the upper part of the photograph. Progressive segregation of biotite and leucosome into differentiated layers is observed in the lower part. The layers are here deformed by F2 folds. (e) Type 1 leucosome. More advanced stage of differentiated layering developing into an actual stromatic structure (left side). Biotite-rimmed K-feldspar augen are locally preserved. Layering is here deformed by F3 folds. Note that veins filled with Type 2 leucosome intruded more or less parallel to the axial planes of the F3 folds. In the central part of the photograph, a small patch of Type 2 leucosome formed in the most highly sheared part of a F3 fold limb (arrowed), thus suggesting that shearing may have enhanced syn-D3 local melting. (f) Wide angle view of the same outcrop. Syn-D1 (Type 1) layering is deformed by F3 folds showing conjugate axial planes (F3′ and F3″). These folds are crosscut by veins filled with Type 2 leucosome. The contacts are sharp. These veins are grossly parallel to the fold axial planes but may be markedly oblique (left-hand side). When parallel with the axial plane of the folds, the veins intruded along either the axial plane or the limb at a low angle to the axial plane. Diffuse granitization (also Type 2 leucosome) occurs in the bottom part of the outcrop without disturbing the stucture. (g) Type 2 leucosome invading F3 folds that have affected the S1 foliation and associated Type 1 layering. The S1 foliation and layering are well preserved in the upper left of the outcrop and appear as a 'ghost foliation' in the granitized area. Preserved K-feldpar augen are frequent. (h) Line drawing of (g) showing the geometry of the F3 folds, which remains undisturbed in the granitized part of the outcrop. Note that these F3 folds have conjugate axial planes and are similar to those in (f).

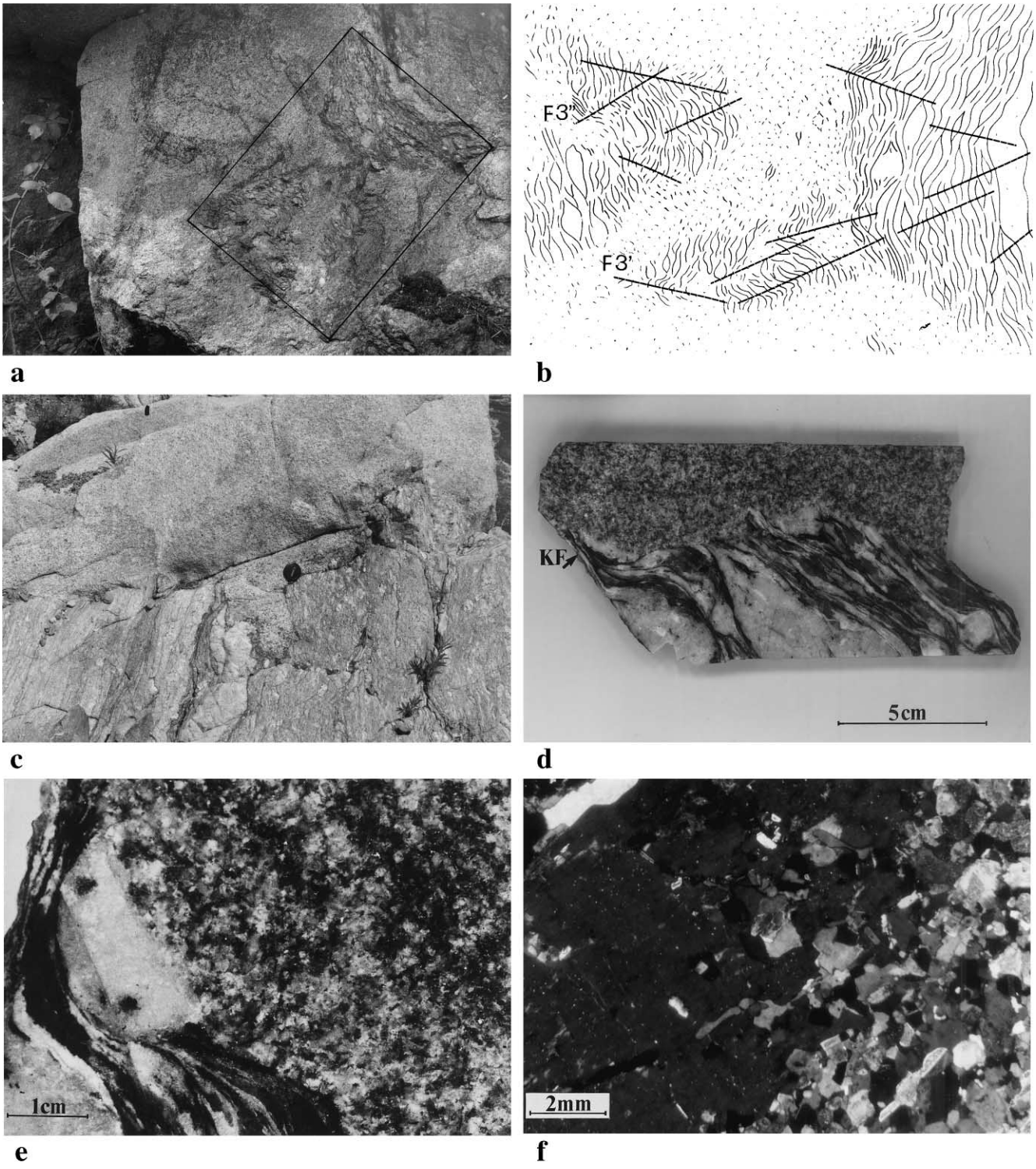

Fig. 6. (a) 'Enclaves' in a Type 2 leucosome. The S1 foliation and the augen structure of the gneisses are preserved in the enclaves and deformed by F3 folds. No Type 1 leucosome formed. Although no ghost foliation is present between the 'enclaves', the similarity in orientation of the S1 foliation and F3 folds show that these enclaves were not disoriented during granitization. (b) Line drawing of the area outlined in (a). The F3 folds show conjugate axial planes ($F3'$ and $F3''$) and their axial planes are in continuity from one enclave to another. (c) Syn- to late-D3 sub-horizontal large dike filled with Type 2 leucosome crosscutting the S1 foliation at a high angle. The contacts are sharp. In the centre of the photograph, the dike bulges more or less parallel to S1 but lacks any continuity with syn-D1 layering only present in the left part of the outcrop. (d) Close-up view of the contact. No continuity appears between the dike and the incipient layering in the gneisses. To the left, a K-feldspar megacryst (KF) seems at first sight to be crosscut by the dike. (e) Close-up view of (d). Sample rotated through 90°. The outline of the megacryst KF remains visible within the granitoid, which precludes an emplacement through an open fracture. (f) Photomicrograph of the 'contact', plane polarized light. Progressive granitization of the KF megacryst. Remnants of K-feldspar in optical continuity with the host are preserved within the granitized part of the megacryst, thus explaining why the contours of the original feldspar are still visible.

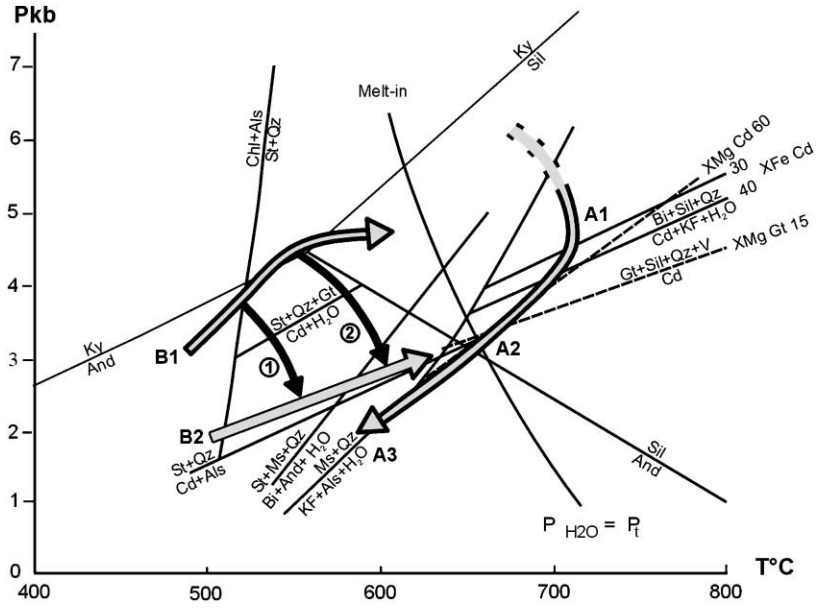

Fig. 7. PT diagram for the gneissic core and the metasedimentary envelope of the Montagne Noire Axial Zone (modified after Ourzik et al. (1991) and Ourzik (1993)). Curve A records the retrogressive metamorphic evolution of the anatectic gneissic core. Point A1 indicates Stage 1 peak metamorphic conditions. Point A2 indicates the transformation of garnet into cordierite. Point A3 represents the crystallization of the most evolved granitoid melts. Curves B1 and B2 refer to the envelope. Curve B1 represents Stage 1 prograde metamorphism. Curve B2 represents Stage 2 retrogressive metamorphic conditions. This curve does not record the PT path of any particular rock volume. Curves 1 and 2 show the PT path of two particular rock volumes arrived at two different PT levels during Stage 1 prograde metamorphism.

The relationship of Type 2 leucosomes with D2 and D3 structures enables us to characterize the granitization process. The veins and dikes frequently contain a 'ghost foliation' inherited from the gneisses and the dikes of large dimensions also include enclaves of poorly transformed or intact gneisses. In most of these dikes, the orientations of the S1 foliation and F2 or F3 folds do not vary particularly from one enclave to another and from enclaves to host rock and the geometric characteristics of the F2 folds are preserved within the wider dikes as well as within the narrower veins (Figs. 5f–h and 6a and b). These features preclude large magmatic flow and melt escape, which is corroborated by the absence of a noticeable preferred mineral orientation other than the ghost foliation.

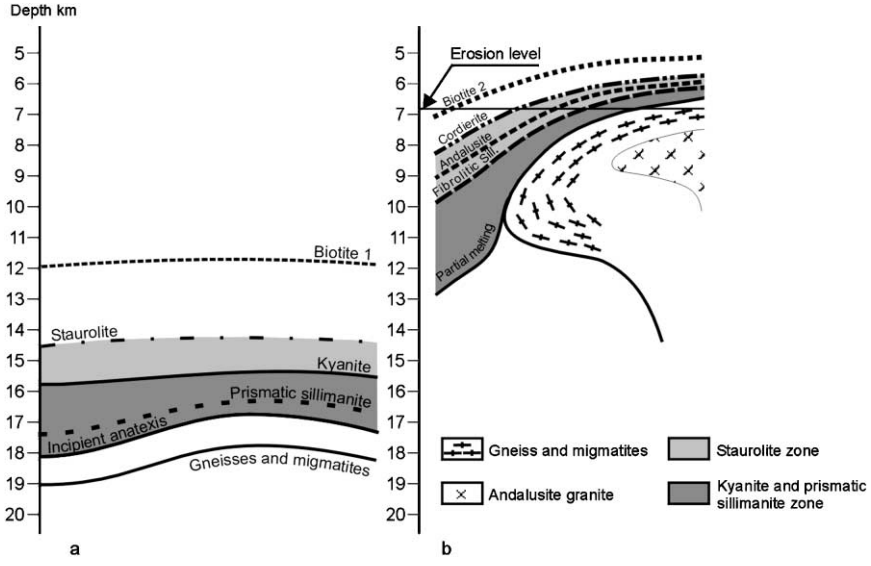

Fig. 8. Schematic evolution of metamorphism and structure in the Montagne Noire Axial Zone. Distances are not to scale. (a) Stage 1 metamorphism. The domal structure is only slightly defined by the shape of the isograds. (b) Stage 2 metamorphism. The domal structure is now well marked. Stage 1 metamorphic zones are deformed and the shape of the Stage 2 metamorphic isograds results from the combination of the tectonic and thermal structures due to the uplift of the anatectic gneissic core. Local deformation of the isograds may result from the emplacement of late granitoids.

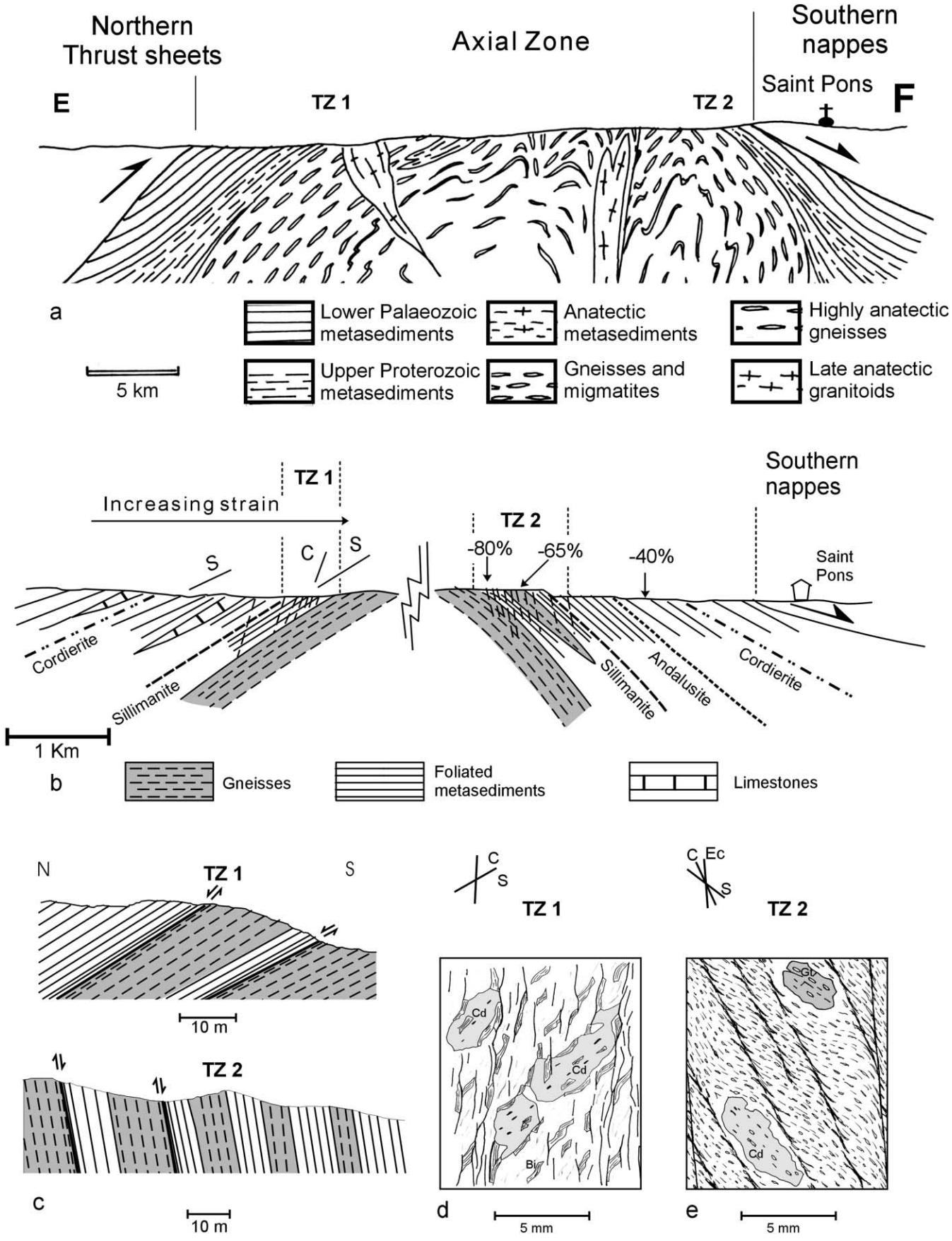
Northern
Thrust sheets
Axial Zone
Southern
nappes
Saint Pons
E
F
TZ 1
TZ 2
a
5 km
Lower Palaeozoic metasediments
Anatectic metasediments
Highly anatectic gneisses
Upper Proterozoic metasediments
Gneisses and migmatites
Late anatectic granitoids
TZ 1
Increasing strain
S
C
S
Southern
nappes
TZ 2
-80%
-65%
-40%
Saint
Pons
Cordierite
Sillimanite
N
Sillimanite
Andalusite
Cordierite
1 Km
b
Gneisses
Foliated metasediments
Limestones
N
TZ 1
S
10 m
TZ 2
c
10 m
C
S
TZ 1
C Ec
S
TZ 2
Cd
Cd
Bi
d
5 mm
Gt
Cd
e
5 mm

Instead, these features suggest in situ melting. Evidence of probable in situ melting is also provided by the granitization of K-feldspar augen at host-rock-dike contacts (Fig. 6c–f). These observations contrast with other migmatitic areas where flow and melt escape structures seem to be more frequent (e.g. Mehnert, 1968; Soula, 1969; Brun, 1975; Brown, 1979; Sawyer, 1996; Brown and Solar, 1998; 1999; Vanderhaeghe, 1999), possibly because of the granitic composition of the protolith.

2.7. Conditions of metamorphism

In the gneissic core, Stage 1 metamorphism corresponds to peak metamorphic conditions, which have been estimated by Ourzik et al. (1991); Ourzik (1993) of ~700° and 5 ± 0.5 Kb (point A1 in Fig. 7), in agreement with the previous estimates made by Schuiling (1960, 1963), Schuiling and de Widt (1962), Den Tex (1975) and Demange (1982). Stage 2 metamorphism indicates lower PT conditions. These PT conditions have been estimated as ~650° and 3 Kb by Ourzik et al. (1991) using the diagrams of Aranovich and Podlesskii (1983) and Perchuk and Lavrent'eva (1983), for X_{Mg} of garnet between 0.12 and 0.15, and X_{Mg} of cordierite between 0.58 and 0.60 (point A2 in Fig. 7). The Stage 1 to Stage 2 PT path (Fig. 7) is similar to those frequently observed in migmatite formations (Palmeri, 1997). Stage 3 metamorphism indicates conditions of ~600° and ~2.5 Kb (Ourzik, 1993) (point A3 in Fig. 7). Taken together, PT data indicate a clockwise P-T-t path in the gneissic core of the Agout Dome (Ourzik et al., 1991; Ourzik, 1993; Gardien et al., 1997) (Fig. 7).

In the envelope, Stage 1 metamorphism represents the peak metamorphic conditions, which may be estimated as ~620°C and 4.5 Kb on the contact with the gneisses, in agreement with Thompson and Bard (1982) (path B1 in Fig. 7). The evolution of the metamorphic conditions from Stage 1 to Stage 2 is constrained by the transformations of staurolite into cordierite and staurolite into andalusite. These transformations indicate that pressure decreased with time while temperature slightly increased (path B2 in Fig. 7). The PTt paths of rock volumes in which these transformations occurred are thus clockwise (e.g. curves 1 and 2 in Fig. 7).

When considering the migmatitic dome and its envelope together, it appears that metamorphism prograded from the micaschists to the anatectic gneisses but with a marked discontinuity at the contact (Fig. 7). The decrease in pressure with time can be interpreted as a result of the common ascent of both formations (Warren and Ellis, 1996) but the discontinuity in pressure and the absence of the incipient melting zone in the envelope at the contact with the gneisses indicates that the gneisses rose higher and/or faster than the envelope (Fig. 8). The timing relationship of deformation and metamorphism/anatexis indicates that uplift occurred more or less continuously from D1 to D3.

2.8. The contact between the gneissic core and the envelope

The contact between the gneissic core and the metasedimentary envelope appears as a 'transition zone' (Gèze, 1949), 150–200 m thick (Fig. 1b), which consists of alternating orthogneissic and metasedimentary sheets with thicknesses of several metres (Debat, 1974; Debat and Vidal, 1981; Cassard et al., 1993; Ourzik, 1993). The rocks are strongly deformed and develop a mylonitic foliation parallel to the contact. Strain estimates in the gneisses and metasediments using the methods of Debat et al. (1975) and Hudleston (1973), yield minimum shortenings of −65 and −80%, respectively. Shear sense criteria such as megacryst rotation, pressure-shadow shapes, shear band asymmetries or S–C fabrics indicate normal-sense displacement at either longitudinal extremity of the dome, with top to the east shear sense to the north-east and opposite shear sense to the south-west (Beaud, 1985; Faure and Cottereau, 1988; Ourzik, 1993; Aerden, 1998). Shear criteria also indicate a component of normal-sense displacement at the north-western and south-eastern margins of the dome, although the main extension is longitudinal (Beaud, 1985; Ourzik, 1993; Aerden, 1998; Debat, unpublished). These observations demonstrate a relative uplift of the gneissic core with respect to the metasedimentary cover, which is consistent with the overall attitude of S1 and S3. When following the evolution of the structures step by step, the regional foliation S1 appears to grade into the S-type mylonitic foliation and the C planes to develop as discrete accentuations of S3 (Fig. 9b). Timing relationships between metamorphic minerals and the mylonitic foliation is best seen in the metapelitic sheets where Stage 2 metamorphic minerals (biotite, andalusite, cordierite and locally sillimanite) are aligned with the mylonitic foliation in the same manner as with S1 outside the contact zone, whereas Stage 3 metamorphic minerals (biotite, fibrolitic sillimanite) are aligned with the C planes (Fig. 9d). These features

Fig. 9. (a) Synthetic cross-section through the Montagne Noire Axial Zone (see location in Fig. 1a). (b) Details of the core-envelope contact to the north-west (left) and to the south-east (right). Strain increases significantly and the regional foliation grades into S/C structures when approaching the contact (TZ = "'transition zone'). Shortening values are inferred from the rotation of feldspar megacrysts (Debat et al., 1975) in the gneisses and from microfolds (Hudleston, 1973) in the metasediments. (c) Outcrop-scale details of the 'transition zone' in the north-western (TZ1) and south-eastern (TZ2) contacts. Only S foliation is represented. Bands with tight lines are higher strain bands in the S/C mylonites. Other ornament as in (b). (d) C/S structures in a metapelite from the northern 'transition zone'. The cordierite crystals (Cd) are aligned with and bounded by the S foliation and include biotite grains aligned either with the S foliation or the C planes. Pressure shadows around the cordierite crystals are generally aligned with the S foliation but their tips are frequently rotated to be aligned with the C planes. (e) C/S structures in a metapelite from the south-eastern contact. Late extensional crenulation (Ec) is also seen cross-cutting the S/C structure. Cd: cordierite; Gt: garnet.

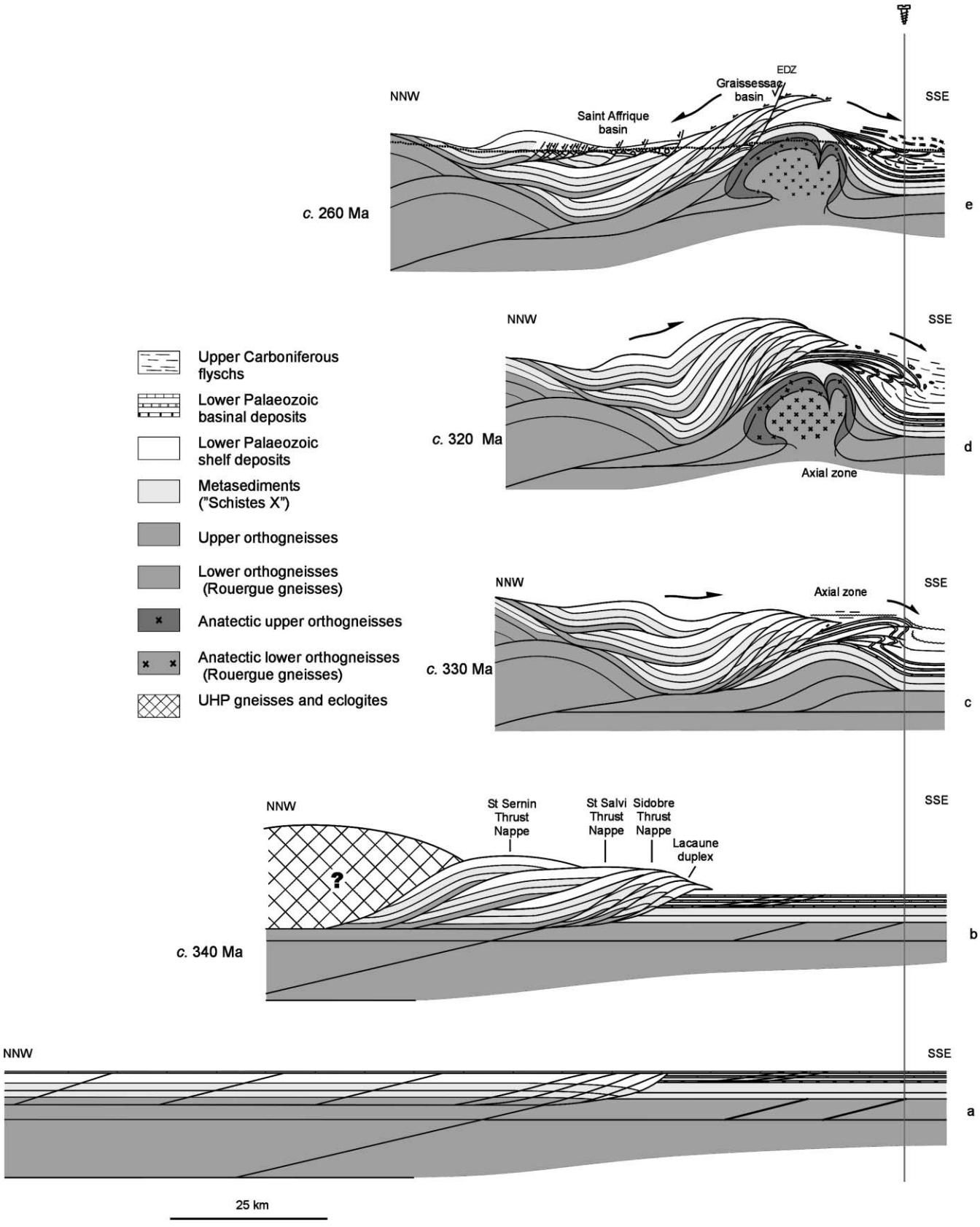
EDZ
Graissessac basin
NNW
SSE
Saint Affrique basin
c. 260 Ma
e
NNW
SSE
c. 320 Ma
d
Axial zone
Upper Carboniferous flyschs
Lower Palaeozoic basinal deposits
Lower Palaeozoic shelf deposits
Metasediments ("Schistes X")
Upper orthogneisses
Lower orthogneisses (Rouergue gneisses)
Anatectic upper orthogneisses
Anatectic lower orthogneisses (Rouergue gneisses)
UHP gneisses and eclogites
NNW
Axial zone
SSE
c. 330 Ma
c
NNW
St Sernin Thrust Nappe
St Salvi Thrust Nappe
Sidobre Thrust Nappe
Lacaune duplex
SSE
?
c. 340 Ma
b
NNW
SSE
a
25 km

indicate that the HT decompression was associated with the relative uplift of the gneissic core.

2.9. Large-scale structures on both sides of the dome

The large-scale structures are not visible in the Axial Zone because of the migmatization but have been well recognized on both sides of the dome owing to a careful mapping (Gèze, 1949; Arthaud, 1970; Donnot and Guérangé, 1978; Engel et al., 1980–1981; Guérangé-Lozes, 1987; Guérangé-Lozes and Burg, 1990). This detailed mapping enabled us to construct a balanced cross-section from the Rouergue to the southern foreland basin (Fig. 10). As in many other balanced cross-sections, layer-parallel ductile shortening, which is essentially represented here by the F2 folds, has not been restored. Since the thickness of the sedimentary pile was also measured in the deformed state, the construction of the section is not altered and the map-scale shortening inferred from the balanced section can be considered as the minimum shortening. In fact, ductile shortening inferred from the analysis of selected F2 folds using the method of Hudleston (1973), and taking into account the distribution of these folds, has not been found greater than −15%. The shortening associated with the S1 foliation is, in contrast, much greater. To account for this, the restoration integrates layer-parallel simple shear, which is thought responsible for the development of S1 at low angles to bedding. For convenience, the shear strain γ has been taken equal to one, which corresponds to a shortening normal to S1 of −0.39%, consistent with the microstructural observations. However, taking higher γ values such as two or three (−59 or −70% shortening) would not have significantly altered the restoration. Another uncertainty could be that the section passes across the Lacaune–Espinouse fault, interpreted as a strike-slip fault by some authors (Demange, 1993; Matte et al., 1998) but as an extensional fault by others (Brun and Van Den Driessche, 1994). As reported above, the map-scale strike-slip displacements are small and the significance of the balanced cross-section cannot be greatly affected. The balanced section integrates Stephano–Permian extension, which can be inferred independently from the study of the Saint Affrique Basin (Legrand, 1990; Legrand et al., 1994) and was responsible for larger map-scale displacements.

To the north of the dome, the upper Proterozoic and lower Paleozoic gneisses, metasediments and unmetamorphosed sediments are involved in south-east vergent fold-and-thrust structures which are, from north to south, the Albigeois duplex, which includes the Saint Sernin and Saint Salvy thrust sheets (the Albigeois nappes of Guérangé-Lozes (1987) and Guérangé-Lozes and Burg (1990)) and the Sidobre thrust sheet (the 'autochtonous' unit of the preceding authors), and the Lacaune duplex, constituted of several steeply dipping and narrow horses (Donnot and Guérangé, 1978) (Fig. 10). The Albigeois duplex and the underlying Rouergue Dome are overthrust by the UHP rocks of the Levezou and Vibal units (Fig. 2).

To the south of the Agout Dome, upper crustal fold and thrust units (the so-called nappes) emplaced into a developing foreland basin in which were deposited turbidites of Late Visean to early Namurian age (Engel et al., 1980–1981; Feist and Galtier 1985). Three major units have been recognized, from north to south: the Minervois–Mont Peyroux, Faugères and Pardailhan 'nappes' (Arthaud, 1970) (Fig. 1c). These units are characterized by flat lying upside-down sequences cropping out over areas of several tens of square kilometres (Gèze, 1949; Arthaud, 1970) (Figs. 1 and 10), which appears to be rather unusual in thrust systems adjacent to foreland basins. The overturned anticlinal hinges have south-dipping axial planes and are associated with south-dipping thrust faults. The dip of the thrust faults decreases progressively when going away from the dome and locally changes from south to north. The relative displacements along these faults are top to the south whatever the direction of the dip. Thrust dips and strata overturning are related to the initial position of the transported material. The more internal the transported unit, the farther its transport into the foreland basin, the higher the dip of the thrusts near the dome and the more pronounced the overturning of the strata (Arthaud, 1970, p. 42). Fossil and sedimentological evidence shows that four successive turbiditic units were deposited in the foreland basin as a result of the successive emplacement of the fold-and-thrust ('nappes') units (Engel et al., 1980–1981; Engel and Franke, 1983). According to these authors (Engel et al., 1980–1981, p. 378; Franke and Engel, 1986), the deposition of each of the turbiditic units occurred in front and on top of each of the fold-and-thrust units as these units progressed southward in

Fig. 10. Balanced cross-sections through the Montagne Noire and surroundings (same section as Fig. 1d). Sequential restoration. Erosion was not shown in stages b to d. Surface data used in this section are those cited in Fig. 1d. The restoration integrates layer-parallel simple shear responsible for the development of the regional foliation S1 at low angle to bedding ($\gamma = 1$). (a) Initial configuration. (b) Development of the Albigeois and Lacaune duplexes. (c) Development of the Rouergue and Montagne Noire antiformal stacks (for convenience, only two 'thick' horses are shown in the Montagne Noire). Fault propagation folds form in the developing foreland basin. (d) Diapiric uplift of the underlying anatectic gneisses resulting from local crustal melting enhanced by antiformal stacking. The stacked horses are strongly deformed at the same time as the upper gneisses are affected by partial melting and the gneissic core pierces its metasedimentary envelope. In the foreland basin, the evolution of the fault propagation folds allowed by the uplift of the basement high arrives at a complete overturning of the short limbs. The upper units are transported farther toward the south, whereas large-scale olistostromes are sliding into the basin. (e) Post-thickening extensional collapse. The diapiric core of the Montagne Noire dome is rotated and gives rise to asymmetrical shear structures. To the north, the thrusts are inverted and new extensional faults form and branch onto the inverted sole thrusts, thus controlling the development of the Graissessac and Saint Affrique basins. To the south, the thrust faults are reactivated by gravitational sliding along the pre-existing thrust faults and the displacements are still top to the south. EDZ is the Espinouse Detachment Zone.

such a way that each tectonic-depositional unit overthrusts the preceding structural unit and related deposits. The fourth depositional unit (known as 'écailles de Cabrières'), which overrides the third structural unit (the Pardailhan 'nappe') is essentially constituted of very large (up to several square kilometres) olistostromes. Many of these olistostromes originated from the disruption of the northern carbonate platform, which shows that this platform was involved in the tectonic process (Engel et al., 1980–1981). Fossils found in shelf carbonate olistoliths transported into the turbidites indicate that the emplacement of the fold-and-thrust units occurred during the Late Visean and the Early Namurian, from the V3bg for the lowest unit (Vachard, 1974; Engel et al., 1980–1981), to at least the V3c E1 (Engel et al., 1980–1981; Feist and Galtier, 1985) and very probably the E2 (E. Poty, oral communication) for the uppermost unit.

Fold and fault structures of this area were previously interpreted as a result of gravity-driven faults crosscutting the overturned limb of a single large-scale recumbent fold refolded by upright folds (Arthaud, 1970; Echtler and Malavieille, 1990). More recently, the recumbent fold was re-interpreted as a late-contractional gravity spreading lobe and the 'nappes' as a result of a younger (Stephano–Permian) collapse (Aerden and Malavielle, 1999). An alternative interpretation which takes into account the results of the sedimentological and paleontological studies mentioned above is preferred here. This interpretation is derived from the model of Specht et al. (1991) and Déramond et al. (1993), for strata and anticlinal hinges overturning during sedimentation in the southern foreland basin of the Alpine Pyrenees. This model, defined as the C.A.S. system (French: *Chevauchement-Anticlinal-Synclinal*, Déramond et al., 1996), is based on the evolution of a syn-sedimentary fault propagation anticline (Suppe and Medwedeff, 1990) in a foreland basin. Strata overturning occurs as a result of the rotation of the forelimb of the fold. When the rotation of the overturned limb becomes mechanically impossible, a new thrust surface develops in the hanging wall anticline. Several new thrust surfaces will thus develop in the hanging wall with an overstep propagation sequence. Applied to the Montagne Noire, this model may explain why folding and overturning of the sediments previously deposited as a result of the emplacement of a lower tectonic unit occurred just before these sediments were overthrust by the succeeding unit, and why strata overturning is related to thrust dip rotation. The ages of emplacement of the successive tectonic-depositional units and the fact that the most internal units are transported farther into the foreland basin bear evidence that an overstep thrust propagation occurred in the Montagne Noire as in the Alpine Pyrenees (Fig. 10c and d). The larger and more evolved structures in the Montagne Noire compared with those in the Alpine Pyrenees can be explained by an over-rise of the basement dome beneath and behind the fault-propagation anticline, which caused a top to the south rotation of the faults during their propagation into the developing foreland basin. Near the dome, the dip of the faults that was initially to the north will be inverted to the south, which makes possible a further rotation of the overturned limbs without changing the sense of the along-fault relative displacement (Fig. 10c and d). At a greater distance from the dome, the faults will be less rotated and, locally, may preserve their dip to the north.

3. Age of the deformations

In the Albigeois, to the north of the Axial Zone, the major regional deformation and associated HT–LP metamorphism, which are related to the development of the fold and thrust structures (Guérangé-Lozes, 1987), have been dated at 346–340 Ma from $^{39}Ar/^{40}Ar$ measurements (Costa and Maluski, 1988). In the Axial Zone, the age of crystallization of the more evolved anatectic magmas that marked the more advanced stage of the HT–LP metamorphism and sealed the development of the dome, has been estimated in the Espinouse dome (Vialais granite) at 327 ± 5 Ma from U/Pb measurements on zircon and monazite (Matte et al., 1998). This estimate is consistent with previous $^{39}Ar/^{40}Ar$ measurements, which have given an age of 316–320 Ma in the Caroux Dome (Maluski et al., 1991) if we consider that these latter ages represent those of cooling rather than those of crystallization. These data are also consistent with previous Rb/Sr ages (Hamet and Allègre, 1976). This means that not only the major deformation D1 — which was broadly synchronous with the first and second metamorphic stages — but also the development of the dome (D2 and D3), were older than 320 Ma. On the southern side of the Axial Zone, the ages of deposition of the syntectonic turbidites range from Late Visean (V3bb–V3c) to Early Namurian ($\leq$V3c-E1–E2) (see above), i.e. between ca. 330 and 320 Ma according to Odin and Odin (1990). Taken together, these age estimates enable us to infer that the development of the foreland basin system and associated thrusting was contemporary with the HT–LP metamorphism and the development of the dome, in spite of the uncertainties arising from the comparison of radiometric and fossil ages. This also shows that, in the studied area, thrusting and associated metamorphism progressed southwards between ca. 340 and 320 Ma.

Younger ages of 308 and 297 Ma have been obtained from $^{39}Ar/^{40}Ar$ measurements in the late shear zones on the southern and northern boundaries of the dome (Maluski et al., 1991). These ages, which are likely to represent those of the end of the metamorphic process, are consistent with those ascribed to the development of the Stephano–Permian basins of Lodève–Graissessac and Saint Affrique (Figs. 1b and 9e) which occurred from the Middle(?) Stephanian to the Thuringian (Rolando et al., 1988), i.e. from ca. 300 to 250 Ma according to Odin and Odin (1990).

4. Discussion

4.1. Mechanism of doming

The main constraints on the interpretation of the Montagne Noire dome are that: (a) doming is accompanied by syn-contractional HT decompression metamorphism, (b) the migmatized orthogneissic core rose faster than the envelope, (c) the deposition of the turbiditic units in the foreland basin was related to the emplacement of fold-and-thrust units (the so-called 'nappes'); and (d) the large-scale structure involves south-vergent fold-and-thrust systems on both sides of the dome. In the following paragraphs, the possible mechanisms will be discussed accordingly. In this discussion, the references indicated at the outset of the sections are those concerned with the interpretation of the Montagne Noire.

4.1.1. Antiformal buckling

Large-scale buckling of a previously flat-lying syn-metamorphic foliation and of a pre-thrusting large-scale recumbent fold (e.g. Arthaud, 1970; Bard, 1978b; Bogdanoff et al., 1984; Laumonier and Marignac, 1996; Demange, 1998; Matte et al., 1998) is consistent with the age of the metamorphic events and with timing relationships between metamorphism and deformation. However, 'post-nappe' doming is rather unlikely because: (a) doming was contemporary with and controlled the emplacement of the thrust sheets into the developing foreland basin, and (b) the existence of a pre-thrusting large-scale recumbent fold is inconsistent with the observed relationship between thrusting and sedimentation. Moreover, pure buckling could hardly agree with the thrust-and-fold structures observed on both sides of the dome and does not explain why the gneissic core and the metasedimentary envelope rose at a different rate. Pure contractional doming can no more explain the HT decompression and the clockwise PTt paths shown by the metamorphic evolution.

4.1.2. Thrust-related doming

Thrust-related doming (e.g. Graham et al., 1987; Matte, 1991) is consistent with the age constraints and is more in accordance with the thrust-and-fold structures observed on both sides of the dome than is large-scale buckling. The interpretation of the Axial Zone dome as an antiformal stack (Fig. 10c) is preferred here to a single large-scale ramp anticline (Graham et al., 1987, fig. 16; Matte, 1991, fig. 5C) because it can account for a probable first-step imbricate thrusting (see Section 2.5), and the subsequent folding of the imbricates. Antiformal stacking of imbricate thrust sheets has been recognized in northwest Spain, in the same foreland of the South European Variscides (Perez-Estáun et al., 1991). However, the antiformal stacks in the latter area are not affected by metamorphism and anatexis and the amplitude/half-wavelength ratio is significantly less than in the Montagne Noire. Although more horses might have been stacked in the Montagne Noire, thrust-related doming alone is not thought sufficient to have provoked the uplift and the increase in slope necessary for strata overturning and thrust dip rotation to occur in the southern units. In any event, thrust related doming alone can no more than buckling explain the differing uplift rates of the core and envelope. On another scale, thrusting alone would have provoked either heating accompanied by burial and counter-clockwise PTt paths or decompression cooling (England and Tompson, 1986; Midgley and Blundell, 1997) instead of high temperature decompression and clockwise PTt paths as actually observed.

4.1.3. Post-thickening extensional collapse

Post-thickening extensional collapse (e.g. Echtler and Malavieille, 1990; Van Den Driessche and Brun, 1991–1992; Brun and Van Den Driessche, 1994, 1996) could be consistent with the observed HT–LP metamorphism and relative uplift of the gneissic core. This interpretation implies, however, that the HT–LP metamorphism was Stephano–Permian in age, which is inconsistent with the radiometric ages of peak metamorphism and anatexis. The age of 327 ± 5 Ma of the late-anatectic (syn-to post D3) granitoids, which seal the domal structure (Matte et al., 1998) is also evidence that this domal structure was largely achieved during regional contraction. However, the development of the Stephano–Permian extensional basins above and to the north of the Montagne Noire (Van Den Driessche and Brun, 1991–1992; Legrand et al., 1991, 1994; Brun and Van Den Driessche, 1994; Burg et al., 1994) shows that post-thickening extensional collapse did occur but as a late- to post-metamorphic process, which is corroborated by the 308 and 297 Ma ages of the late shear zones (Maluski et al., 1991). The objection to the master fault of the extensional system being a vertical fault showing dextral or dextral-normal displacements and not an extensional listric fault (Demange, 1993; Matte et al., 1998) can hardly be sustained because the component of transcurrent shearing inferred from microtectonic markers did not give rise to large map-scale displacements, whereas much larger extensions have been inferred from the study of the basins ($\geqq 6$ km, Legrand, 1990; >15 km, Burg et al., 1994). Most of this extension is likely to have been accommodated by the negative inversion of thrust faults (Legrand et al., 1994).

4.1.4. Syn-contractional gravitational collapse

Syn-contractional gravitational collapse of the metasedimentary cover of the gneisses and consecutive denudation of the gneisses giving rise to HT decompression metamorphism (Aerden, 1998; Aerden and Malavielle, 1999) is apparently consistent with the succession of the microstructural events in the Axial Zone but can hardly be retained:

1. The HT–LP (Stages 1–3) metamorphism was contemporary with the late Visean–early Namurian turbidites and

with the fold-and-thrust structures that controlled the deposition of these turbidites in the foredeep.
2. The fold and thrust structures have the same vergence and style on both sides of the dome.
3. The fold and thrust structures in the Upper Palaeozoic developed in continuity with the fold-and-thrust structures in the Lower Paleozoic of the northern area, which means that the contractional deformation occurred at the same time in the upper as in the lower levels.

On another ground, a late (Stephano–Permian) emplacement of the so-called nappes in the form of a gravity-spreading lobe (Aerden and Malavielle, 1999) is inconsistent with the observed tectonics–sedimentation relationship but it is likely that pre-existing thrusts were reactivated by the late-extensional collapse in the southern as well as in the northern units (Brun et al., 1994; Legrand et al., 1994).

4.1.5. Diapirism

Diapirism (Den Tex, 1975; Debat and Vidal, 1981; Beaud, 1985; Faure and Cottereau, 1988; Ourzik, 1993) is capable of explaining both high temperature decompression and higher uplift rate of the gneissic core as inferred from the study of metamorphism. The possibility of diapirism will then be discussed on the basis of the physical and structural data relevant to the studied area.

The *physical possibility* of diapiric ascent of liquid granitic magmas has been much debated for the last 10 years in the community of granite researchers (e.g. Clemens and Mawer, 1992; Petford, 1996; Clemens et al., 1997; Clemens and Droop, 1998 on one side and Weinberg, 1996; Paterson and Miller, 1998; Kosakowski et al., 1999, on the other side), but little has been written on the physical possibility of solid state diapirism (see, however, Talbot and Koyi, 1995 or De Bremond d'Ars et al., 1999). The strongest bases for discussing this problem remain either fluid dynamics analyses (Ramberg, 1981, pp. 56–194; De Bremond d'Ars et al., 1999) or correctly scaled analog or numerical models. The analog models of Ramberg (1967, 1981) and similar ones developed in the seventies have been preferred here as they have the advantages of being carefully scaled and presenting a variety of cases more instructive for the present purpose than most of the more sophisticated but restrictive models presented since then. As computed by Ramberg (1981, pp. 100–103) and shown by the models (e.g. Ramberg, 1981, pp. 248, 304; Soula, 1982, p. 334), density differences of 100 to 200 kg m^{-3} are sufficient for diapirism to occur, provided that the effective viscosity is sufficiently low to allow ductile deformation and the viscosity ratio not too high ($\sim 10^3$ to 10^{-3}). In metamorphosed rocks, density must be estimated in the PT conditions under which diapirism is suspected to have occurred. Density estimates of solid rock formations need to take into account the thermal expansion and compressibility of the rock-forming minerals (data in Skinner (1966) and Robie et al. (1966)) and the relative abundance of the different rock-types in a given formation (e.g. Soula, 1982). Compressibility can, however, be ignored here as it only slightly changes the density of solids in the range of pressures considered (see Soula, 1982, fig. 17). In the case of partially molten rocks, melt densities have been computed using the methods of Bottinga et al. (1982) for the oxide components and Burnham and Davis (1971, 1974) for water. Minimum water contents of the melts have been determined using fig. 2 of Holtz and Johannes (1994). Rock plus melt densities have been computed taking into account: (a) the quantity and composition of the different leucosomes, and (b) the composition of the paleosome deprived of the mineral portion extracted to form the leucosomes. Using this method, the density of the biotite and andalusite-rich envelope of the Agout Dome at 700°C has been estimated to about 2790–2840 kg m^{-3} and the density of the unmelted granitic gneisses of the core at the same temperature to about 2580–2590 kg m^{-3}. The difference in density between the core and the envelope is then of 200–260 kg m^{-3}, which would be sufficient by itself to allow diapiric ascent. The estimated density of partially molten gneisses are given in Table 1 for differing amounts of Type 1 and Type 2 leucosomes. These calculations show that in all cases, the density of the solid and hydrated melt is lower than the density of the protolith. As in other migmatites, it is difficult to estimate the average melt content of the entire formation. However, if we consider only Type 1 leucosomes, which are present all within the core in proportions varying between ~5 and $\geqq$ 30%, the average content may be reasonably estimated to be about 15–20%. The average content of Type 2 leucosomes might be estimated to be about 10%. As a result, the density of the partially molten gneisses may be estimated to about 2500–2530 kg m^{-3} during D1 (melt present but no

Table 1
Density of melts, solid plus melt and solid at 700°C in the migmatized granitic orthogneisses of the Montagne Noire (in kg m^{-3}). Minimum water content estimated after Holtz and Johannes (1994, fig. 2). Melt densities calculated using the partial molar volume of silicate-melt oxide components (Bottinga et al., 1982) and the partial molar volume of H_2O in the melt (Burnham and Davis, 1971, equation (9)). Density of solids computed using density and thermal expansion of minerals (data after Skinner (1966) and Robie et al. (1966)). Compositions of leucosomes and solid rocks given in the text

Volume melt	100%	25%	20%	15%	10%	5%	0%
Type 1 leucosome (500 MPa)	2184	2487	2506	2528	2546	2569	2589
Type 2 leucosome (250 MPa)	2132	2475	2497	2520	2543	2520	2589
	2137	2476	2499	2521	2544	2521	2589

leucosomes cristallized) and to about 2540–2545 kg m^{-3} during D2/D3 (Type 1 leucosome crystallized but not Type 2). The differences in density between the partially molten gneisses and the envelope are thus about 245–340 kg m^{-3}, which is more than required to allow diapiric uplift.

An objection to diapirism of partially molten rocks is that melt will necessarily escape, thus increasing the density of the melt-depleted rocks (Clemens and Droop, 1998). The observations reported above show that, in the Montagne Noire, melting was essentially in situ, and melt escape structures are rare if not absent, even in the large Type 2 dikes. Moreover, the markedly different composition and the younger age of the large Type 2 dikes are evidence that they cannot have acted as drainage conduits for syn-D1 melts. Although it might be envisaged that a part of the melt infiltrated pre-existing structures without disturbing them (Mehnert, 1968, p. 323; Brown and Solar, 1998), the fact that leucogranitic massifs are absent in the envelope and not particularly abundant near the contact demonstrates that no melt originating from the gneisses escaped out of these gneisses.

Viscosity is more difficult to estimate than density. Effective viscosity ratios between metasediments and migmatized gneisses similar to those in the Montagne Noire were estimated by Soula (1982, fig. 18) from a comparison between the strength of mica-rich solid rocks deformed at high temperature and the strength of partially molten granites in the well-known experiments of van der Molen and Paterson (1979) (melt fractions lower than the 'Critical Melt Fraction'). This gave gneiss-envelope viscosity ratios of 10^2 for 0 vol% melt, 10^{-1} for 20 vol% melt and 10^{-3} for 25 vol% melt, which lay in the range of values (10^3 to 10^{-3}) required for diapiric deformation. Since then, the existence of the CMF has been questionned and other experiments have shown that the strength of the rock may decrease linearly rather than dramatically with increasing melt fraction (Rushmer, 1995, 1996; Rutter and Neumann, 1995). Accordingly, a strength ratio of 10^{-3} between the partially molten gneisses and the envelope can be considered as a maximum and values of $\sim 10^{-1}$ can be more reasonably expected for the observed melt fractions. In fact, there is no structural evidence in the Montagne Noire that migmatization considerably reduced the strength of the gneisses as shown, for example, by the shapes and amplitude-wavelength ratios of the F2 and F3 folds, which are similar in the unmelted and partially molten gneisses (compare Fig. 5f with Figs. 5g and h and 6a and b). Independent lines of evidence of low strength contrast between the core and the envelope are also: (a) the similar shape of the F2 and F3 folds in both formations, and (b) the shortening values estimated in the interlayered gneissic and metasedimentary sheets of the contact zone, which are rather close to each other.

The *structural data*indicate a normal-sense displacement at the core-cover interface all around the dome, which implies a relative uplift of the core that can hardly be interpreted simply in terms of regional gravitational flattening. Moreover, the curvature of the F2 fold axes and L2/L3 stretching lineations and the attitude of S3, which is horizontal and parallel to S1 in the roof and dips steeper than the same S1 in the flanks of the dome, are evidences that S3 formed with an overall domal shape. The presence of flattening-type strain ellipsoids on the roof, together with stretching lineations and upright folds sub-parallel to the contours of the dome in the cover, demonstrates radial expansion of the gneissic core causing radial shortening and concentric extension in the cover. Similar features resulting from radial expansion of diapirs have been observed on top views of analog models (e.g. Ramberg, 1981, pp. 279, 299, 312, 392). Lineations parallel to the contours of the dome associated with shear criteria indicating an uplift of the core have been observed in natural diapiric domes in various contexts (e.g. Bouhallier et al., 1995, fig. 5; Talbot and Koyi, 1995, fig. 7; Dirks et al., 1997, fig. 4; Hippertt and Davis, 2000, fig. 2). In elongate diapirs, the *X* axis of the strain ellipsoids will be sub-parallel to the long axis of the dome if the elongate shape is a result of greater expansion in one direction when the resistance of the overburden is less parallel to pre-existing or developing tectonic structures, i.e. perpendicular to regional contraction (e.g. Ramberg, 1981, pp. 298, 302, 392). In the Montagne Noire, syn-diapiric regional contraction is indicated by the presence of F2 upright folds within the core and can be supported by a comparison between the Montagne Noire and a graphically shortened experimental dome (Fig. 11).

Therefore, density and viscosity data indicate that diapirism was physically possible and the metamorphic and structural data that this process effectively contributed to the development of the Montagne Noire dome. However, as shown above, diapirism was here syn-contractional and cannot be considered independently of the other contributing processes, which are thrusting and post-contractional collapse. Diapirism may explain the additional uplift, which induced strata overturning and thrust dip rotation in the southern fold-and-thrust units. The pre-existence of a diapiric kernel is also likely to have rendered much easier the internal rotation ('roll under' of Brun and Van Den Driessche, 1994) of the Axial Zone during the post-contractional extension. Conversely, antiformal stacking may have enhanced diapirism by creating the initial bulge favoring the initiation of the diapir (Ramberg, 1981, pp. 252–254). The structural sections (Figs. 2 and 10) also suggest that isotherm upwelling at the origin of HT–LP metamorphism and diapirism could have been enhanced by a local over-thickening due to the superposition of an antiformal stack on top of a lower crustal ramp anticline. Over-thickening might have been particularly efficient here because of lithospheric thinning predating regional shortening (Midgley and Blundell, 1997, fig. 9c).

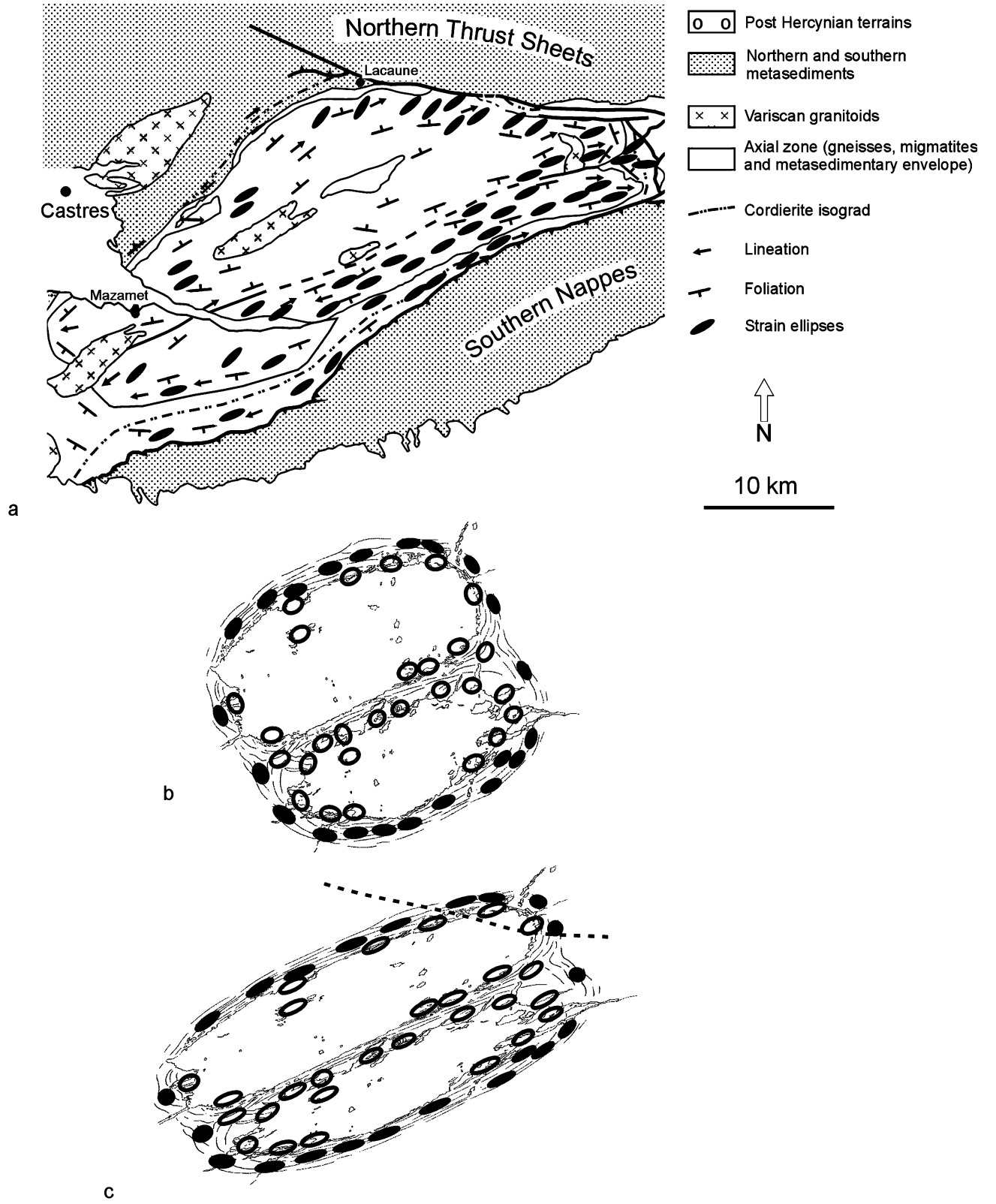

Fig. 11. Comparison of strain ellipses in the Montagne Noire and in a graphically deformed experimental dome. (a) Strain ellipses in the Montagne Noire after Faure and Cottereau (1988), Ferret (1983), Beaud (1985), Brunel and Lansigu (1997) and Mattauer et al. (1996). (b) Strain ellipses constructed from an analogue model of a double diapiric dome (fig. 11-82 in Ramberg, 1981). Solid ellipses constructed from folds and associated extension fissures in the envelope (*XY* planes dips >45°). Open ellipses constructed from the extension fissures in the cover of the core roof. (c) The same, deformed graphically, plane strain, 30% shortening perpendicular to dome axis, no area change.

4.2. The place of the Montagne Noire in the orogenic wedge and foreland basin system of the South European Variscides

The balanced sections presented in the present paper (Figs. 2 and 10) confirm that the Montagne Noire ridge was included in the south-vergent orogenic wedge of the South European Variscides, though situated 200–250 km away from the suture and was not a result of an intracontinental subduction:

1. The UHP continental rocks and eclogites override the wedge from the Haut–Allier suture to the Levezou dome at 60 km to the Montagne Noire.
2. The wedge is exclusively formed of meso- to upper crustal rocks and no other exhumed UHP rocks are seen.
3. All the structures in the wedge are south-vergent, whereas an intracontinental subduction would have probably developed backthrusting.

The width of the wedge is in fact of the same order of magnitude as in other parts of the South European Variscides (see Engel and Franke, 1983; Matte, 1991; Perez-Estáun et al., 1991) or in the Himalayan belt, which has dimensions and an overall geometry in several respects similar to the Variscan belt (Matte, 1991). The essential difference with basement-involved frontal antiformal stacks of younger orogens such as the Alps or Himalayas (see e.g. Roure et al., 1990; Burkhard and Sommaruga, 1998; DeCelles et al., 1998) or other parts of the Variscan belt (e.g. Perez-Estáun et al., 1991), is only that the Montagne Noire antiform was affected by local syn-contractional metamorphism and anatexis, allowing mid- to upper crustal diapirism.

5. Conclusion

The Montagne Noire can be considered as a particular type of basement-involved frontal culmination in an –ordinary– contractional orogenic wedge and associated foreland basin system as defined by DeCelles and Giles (1996). The only, though essential, differences between this frontal culmination and –ordinary– frontal culminations are: (a) the occurrence of a local syn-contractional isothermal decompression metamorphism, and (b) widespread strata overturning in fold-and-thrust sheets that were emplaced into the developing foredeep. The data reported in the present paper lead us to the conclusion that these unusual characteristics resulted from the contribution of three major processes acting sequentially (Fig. 10):

1. Antiformal stacking resulting from forward propagation of fold-and-thrust structures (Fig. 10b and c) during regional metamorphism. The antiformal stack was responsible for a local increase in pressure and crustal thickening of a previously thinned lithosphere, which enhanced local partial melting (Midgley and Blundell, 1997) and further development of the ridge by diapiric rise in the middle to upper crust. Antiformal stacking and related thrust-propagation folds (C.A.S. system, Déramond et al., 1996) controlled the first stages of the foreland basin development and the deposition of the first turbiditic units (Fig. 10c).
2. Diapiric rise of the anatectic granitoid-rich upper basement (Fig. 10d). Diapirism was essentially responsible for the HT decompression recorded by the clockwise PTt paths and is likely to have transported upwards the 'relatively low pressure eclogites' (9 ± 2 Kb, Demange, 1985) previously uplifted by pre-anatectic thrusting. Diapiric rise is also likely to have increased the amplitude, and thus the relative altitude, of the basement high behind the developing foreland basin and is thus believed to have been in a large part responsible for the unusually widespread strata overturning, which characterizes this area. The deposition of the upper turbiditic units occurring during the emplacement of the last thrust units was related to this stage.
3. Extensional doming resulted from late- to post-metamorphic extensional collapse acting on a pre-existing high-amplitude dome (Fig. 10e). Post-thickening collapse is thought to have been responsible for the development of the Stephano–Permian continental basins on top and to the north of the dome and for the extensional reactivation of pre-existing thrusts in the southern units. The asymmetry of the syn-extensional structures are thought to have resulted from the internal rotation of the diapiric core of the pre-existing dome according to a modified version of the 'roll-under' model of Brun and Van Den Driessche (1994). Extension probably proceeded together with a limited dextral transcurrent shearing, possibly related to a counterclockwise rotation of the pre-existing thrust-induced horses as strike-slip dominoes (Cogné et al., 1990, 1993; Diego-Orozco and Henry, 1998).

The apparent differences between the Montagne Noire ridge and 'ordinary' frontal ridges of orogenic wedges are therefore interpreted as consequences of diapirism and related syn-contractional HT–LP decompression metamorphism. It is suggested that the occurrence of these phenomena in front of an orogenic wedge was the result of a local over-thickening due to the superposition of an upper crustal antiformal stack on top of a lower crustal ramp anticline and responsible for a localized uplift of the isotherms in higher levels of the upper crust.

Acknowledgements

We thank Pierre Béziat, Pierre Courjault-Radé,

Jacqueline Guérangé-Lozes and Francis Tollon for helpful discussions and unpublished information relating to regional stratigraphy, tectonics and metamorphism. We are grateful to an anonymous referee for useful and constructive comments on an early draft of this article. Particular thanks go to Richard Lisle for his helpful editorial comments.

References

Aerden, D.G.A.M., 1998. Tectonic evolution of the Montagne Noire and a possible orogenic model for syncollisional exhumation of deep rocks, Variscan belt, France. Tectonics 17 (1), 62–79.

Aerden, D.G.A.M., Malavielle, J., 1999. Origin of a large-scale fold nappe in the Montagne Noire, Variscan belt, France. Journal of Structural Geology 21, 1321–1333.

Allmendinger, R.W., Sharp, J.W., Von Tish, D., Serpa, L., Kaufman, S., Oliver, J., Smith, R.B., 1983. Cenozoic and Mesozoic structure of the eastern Basin and Range Province, Utah, from COCORP seismic reflection data. Geology 11, 532–536.

Aranovich, L.Ya., Podlesskii, K.K., 1983. The cordierite–garnet–sillimanite–quartz equilibrium: experiments and applications. In: Saxena, S.K. (Ed.). Kinetics and Equilibrium in Minerals Reactions. New York: Springer-Verlag, pp. 173–198.

Arthaud, F., 1970. Etude tectonique et microtectonique comparée de deux domaines hercyniens: les nappes de la Montagne Noire (France) et l'anticlinorium de l'Iglesiente (Sardaigne). Thesis, University of Montpellier.

Audren, C., Triboulet, C., 1993. P-T-t deformation paths recorded by kinzigites during diapirism in the western Variscan belt (Golfe du Morbihan, southern Brittany, France). Journal of Metamorphic Geology 11 (3), 337–356.

Bard, J.P., 1978a. Une nouvelle interprétation sur l'origine et l'âge relatif des gneiss oeillés de la Zone Axiale de la Montagne Noire et ses conséquences tectoniques. Comptes Rendus de l'Académie des Sciences de Paris 278, 65–68.

Bard, J.P., 1978b. A propos du style tectonique de la phase hercynienne "précoce" de la Zone Axiale de la Montagne Noire (Massif Central). Comptes Rendus de l'Académie des Sciences de Paris 287, 1321–1324.

Bard, J.P., 1979. Existence d'une suite granitique alcaline d'âge paléozoïque inférieur dans la Zone Axiale de la Montagne Noire (Massif Central français) et ses abords immédiats. Comptes Rendus de l'Académie des Sciences de Paris 288, 371–374.

Bard, J.P., Loueyit, J., 1978. Sur l'origine des gneiss oeilllés de l'Espinouse dans la Zone Axiale de la Montagne Noire (Massif Central): conséquences tectoniques. Bulletin de la Société géologique de France 20, 751–772.

Beaud, F., 1985. Etude structurale de la Zone Axiale orientale de la Montagne Noire (sud du Massif Central français). Détermination des mécanismes de déformation. Thesis, University of Montpellier.

Bodinier, J.L., Giraud, A., Dupuy, C., Leyreloup, A., Dostal, J., 1986. Caractérisation géochimique des métabasites associées à la suture méridionale hercynienne: Massif central français et Chamrousse (Alpes). Bulletin de la Société Géologique de France 1, 115–123.

Bogdanoff, S., 1969. Sur la sillimanite de la zone axiale de la Montagne Noire (Monts de l'Espinous, Hérault). Comptes Rendus de l'Académie des Sciences de Paris 268, 2163–2166.

Bogdanoff, S., Donnot, M., Ellenberger, F., 1984. Notice explicative de la feuille Bédarieux au 1/50,000: Carte Géologique de la France, B.R.G.M., 105pp.

Bottinga, Y., Weill, D., Richet, P., 1982. Density calculations for silicate liquids, I. Revised method for aluminosilicate compositions. Geochimica and Cosmochimica Acta 46, 909–919.

Bouhallier, H., Chardon, D., Choukroune, P., 1995. Strain patterns in Archean dome-and-basin structures: the Dharwar craton (Karnataka, south India). Earth and Planetary Science Letters 135, 5–75.

Brown, M., 1979. The petrogenesis of the St. Malo Migmatite Belt, Armorican Massif, France, with particular reference to the diatexites. Neues Jahrbuch fur Mineralogie Abhandlungen 135, 48–74.

Brown, M., Solar, G.S., 1998. Granite ascent and emplacement during contractionzal deformation in convergent orogens. Journal of Structural Geology 20, 1365–1393.

Brown, M., Solar, G.S., 1999. The mechanism of ascent and emplacement of granite magma during transpression: a syntectonic granite paradigm. Tectonophysics 312, 1–33.

Brun, J.P., 1975. Contribution à l'étude d'un dôme gneissique: le dôme de St. Malo (Massif Armoricain). Analyse de la déformation. Thesis, University of Rennes.

Brun, J.P., Van Den Driessche, J., 1994. Extensional gneiss domes and detachment fault systems: structure and kinematics. Bulletin de la Société géologique de France 165, 519–530.

Brun, J.P., Van Den Driessche, J., 1996. Réponse à observations et remarques sur l'article "Extensional gneiss domes and detachment fault systems: structure and kinematics" (Brun, J.-P., Van Den Driessche, J., 1994. Bull. Soc. géol. Fr. 165 (6), 519–530). Bulletin de la Société géologique de France 167 (2), 295–302.

Brun, J.P., Soukoutis, D., Van Den Driessche, J., 1994. Analogue modeling of the detachment fault systems and core complexes. Geology 22, 319–322.

Brunel, M., Lansigu, Ch., 1997. Déformation et cinématique de mise en place du dôme de la zone axiale de la Montagne Noire: signification des nodules à quartz-sillimanite (Massif central français). Comptes Rendus de l'Académie des Sciences de Paris 325, 517–523.

Burg, J.P., Delor, C., Leyreloup, A., Romney, F., 1989. Inverted metamorphic zonation and Variscan thrust tectonics in the Rouergue area (Massif central, France): P-T-t record from mineral to regional scale. In: Daly, J.S., Cliff, R.A., Yardley, B.W.D. (Eds.). Evolution of Metamorphic Belts. Geological Society Special Publication 43, pp. 423–439.

Burg, J.P., Van Den Driessche, J., Brun, J.P., 1994. Syn- to post-thickening extension in the Variscan Belt of Western Europe: modes and structural consequences. Géologie de la France 3, 33–51.

Burnham, C.W., Davis, N.F., 1971. The role of H_2O in silicate melts: I. P-V-T relaions in the system $NaAlSi_3O_3$-H_2O to 10 kilobars and 1000°C. American Journal of Sciences 270, 54–79.

Burnham, C.W., Davis, N.F., 1974. The role of H_2O in silicate melts: II. Thermodynamic and phase relations in the system $NaAlSi_3O_3$-H_2O to 10 kilobars, 700 to 1100°C. American Journal of Sciences 274, 902–940.

Burkhard, M., Sommaruga, A., 1998. Evolution of the western Swiss Molasse basin: structural relations with the Alps and the Jura belt. In: Mascle, A., Puigdefàbregas, C., Luterbacher, H.P., Fernàndez, M. (Eds.). Cenozoic Foreland Basins of Western Europe. Geological Society Special Publication 134, pp. 279–298.

Calvert, A.T., Gans, Ph.B., Amato, J.M., 1999. Diapiric ascent and cooling of a sillimanite gneiss dome revealed by (super 40)Ar/(super 39)Ar thermochronology; the Kigluaik Mountains, Seward Peninsula, Alaska. Geological Society Special Publications 154, 205–232.

Cassard, D., Feybesse, J.L., Lescuyer, J.L., 1993. Variscan crustal thickening, extension and late overstacking during the Namurian–Wesphalian in the western Montagne Noire (France). Tectonophysics 222, 33–53.

Chardon, D., Choukroune, P., Jayananda, M., 1998. Sinking of the Dharwar Basin (South India): implications for Archaean tectonics. Precambrian Research 91, 15–39.

Choukroune, P., Bouhallier, H., Arndt, N.T., 1995. Soft lithosphere during periods of Archean crustal growth or reworking. In: Coward, M.P., Ries, A.C. (Eds.). Early Precambrian Processes. Geological Society Special Publication 95, pp. 67–86.

Clemens, J.D., Mawer, C.K., 1992. Granitic magma transport by fracture propagation. Tectonophysics 204, 339–360.

Clemens, J.D., Petford, N., Mawer, C.K., 1997. Ascent mechanisms of

granitic magmas: causes and consequences. In: Holness, M. (Ed.). Deformation-Enhanced Fluid Transport in the Earth's Crust and Mantle. Chapman & Hall, London, pp. 144–171.

Clemens, J.D., Droop, G.T.R., 1998. Fluids. *P–T* paths and the fates of anatectic melts in the Earth's crust. Lithos 44, 21–36.

Cogné, J.P., Brun, J.P., Van Den Driessche, J., 1990. Paleomagnetic evidences for rotation during Stephano–Permian extension in the southern Massif central (France). Earth and Planetary Sciences Letters 101, 272–280.

Cogné, J.P., Van Den Driessche, J., Brun, J.P., 1993. Syn-extension rotations in the Permian St-Affrique Basin (Massif central, France): paleomagnetic constraints. Earth and Planetary Sciences Letters 115, 29–42.

Costa, S., Maluski, H., 1988. ^{40}Ar-^{39}Ar dating for terranes boundaries definition. The example of French Massif Central. I.G.C.P. project no. 233. International Conference, Montpellier (France). Abstracts, p. 17.

Courjault-Radé, P., 1985. Comparaison de l'évolution sédimentaire de séquences du Cambrien inférieur et moyen (p.p.) dans les versants sud et nord (unité de Brusque) de la Montagne Noire (Massif central). Comptes Rendus de l'Académie des Sciences de Paris 301, 43–48.

Davis, G.H., Coney, P.A., 1979. Geologic development of the Cordilleran metamorphic core complexes. Geology 7, 120–124.

Debat, P., 1974. Essai sur la déformation des gneiss de la Montagne Noire occidentale. Thesis, University of Toulouse III.

Debat, P., Vidal, J.L., 1981. Essai sur la déformation des orthogneiss (exemples pris dans la Montagne Noire occidentale). Mémoires de la Société géologique de France, nouvelle série 60, 1–70.

Debat, P., Déramond, J., Soula, J.C., 1971. Origine de la structure oeillée dans les gneiss de la Montagne Noire occidentale. Comptes Rendus de l'Académie des Sciences de Paris 272, 2759–2762.

Debat, P., Sirieys, P., Déramond, J., Soula, J.C., 1975. Paléodéformation d'un massif orthogneissique. Tectonophysics 28, 159–183.

De Bremond d'Ars, J., Lécuyer, Ch., Reynard, B., 1999. Hydrothermalism and diapirism in the Archean: gravitational instability constraints. Tectonophysics 304, 29–39.

DeCelles, P.G., Giles, K.A., 1996. Foreland basin systems. Basin Research 8, 105–123.

DeCelles, P.G., Grehels, G.E., Quade, J., Ojha, T.P., 1998. Eocene–early Miocene foreland basin development and the history of Himalayan thrusting, western and central Nepal. Tectonics 17, 741–765.

Delor, C., Burg, J.P., Clarke, G., 1991. Relations diapirisme-metamorphisme dans la province de Pilbara (Australie occidentale): implications pour les régimes thermiques et tectoniques à l'Archéen. Comptes Rendus de l'Académie des Sciences de Paris 312, 257–263.

Demange, M., 1982. Etude géologique du Massif de l'Agout, Montagne Noire, France. Thesis, University of Paris VI.

Demange, M., 1985. The eclogite-facies rocks of the Montagne Noire, France. Chemical Geology 50, 173–188.

Demange, M., 1993. Que signifie la faille des Monts de Lacaune (Montagne Noire, France)? Implications quant au problème de la patrie des nappes. Compte Rendus de l'Académie des Sciences de Paris 317, 411–418.

Demange, M., 1996. Observations et remarques sur l'article "Extensional gneiss domes and detachment fault systems: structure and kinematics" (Brun, J.P., Van Den Driessche, J., 1994. Bulletin de la Société géologique de France 165, 519–530) et réponse de J.P. Brun et J. Van Den Driessche. Bulletin de la Société géologique de France 167, 295–302.

Demange, M., 1998. Contribution au problème de la formation des dômes de la zone axiale de la Montagne Noire: analyse des plissements superposés dans les séries métasédimentaires de l'enveloppe. Implications pour tout modèle géodynamique. Géologie de la France 4, 1–56.

Den Tex, E., 1975. Thermally mantled gneiss domes: the case for convective heat flow in more or less solid orogenic basement. In: Progress in Geodynamics. Royal Netherland Academy Arts Sciences Amsterdam, pp. 62–79.

Déramond, J., Souquet, P., Fondecave-Wallez, M.J., Specht, M., 1993. Relationship between thrust tectonic and sequence stratigraphy in foredeeps: Model and examples from the Pyrenees (Cretaceous-Eocene, France, Spain). In: Williams, G.D., Dodd, A. (Eds.). Tectonics and Seismic Sequence Stratigraphy. Geological Society Special Publication 71, pp. 193–219.

Déramond, J., Delcaillau, B., Souquet, P., Angelier, J., Chu, H.T., Lee, J.F., Lee, T.Q., Liew, P.M., Lin, T.S., Teng, L., 1996. Signatures de la surrection et de la subsidence dans les bassins d'avant-chaîne actifs: les Foothills de Taiwan (de 8 Ma à l'Actuel). Bulletin de la Société Géologique de France 167, 111–123.

Diego-Orozco, A., Henry, B., 1998. Données paléomagnétiques du bassin permien de Rodez et rotations dans la bordure sud-ouest du Massif central. Comptes Rendus de l'Académie des Sciences de Paris 327, 225–229.

Dirks, P.H.G., Zhang, J.S., Passchier, C.W., 1997. Exhumation of high-pressure granulites and the role of lower crustal advection in the North China Craton near Datong. Journal of Structural Geology 19, 1343–1358.

Donnot, M., Guérangé, B., 1978. Le synclinorium cambrien de Brusque. Implications stratigraphiques et structurales dans les Monts de l'est de Lacaune (Tarn, Aveyron, Hérault) — versant nord de la Montagne Noire. Bulletin du BRGM France 2 (1–4), 333–363.

Ducrot, J., Lancelot, J.R., Reille, J.L., 1979. Datation en Montagne Noire d'un témoin d'une phase majeure d'amincissement crustal caractéristique de l'Europe prevarisque. Bulletin de la Société géologique de France 4, 501–505.

Echtler, H., Malavieille, J., 1990. Extensional tectonics, basement uplift and Stephano–Permian collapse basin in a late Variscan metamorphic core complex (Montagne Noire, Southern Massif Central). Tectonophysics 177, 125–138.

Engel, W., Franke, W., 1983. Flysch sedimentation: its relation to tectonism in the European variscides. In: Martin, H., Edel, F.W. (Eds.). Intracontinental Fold Belts. Springer Verlag, Berlin, pp. 289–321.

Engel, W., Feist, R., Franke, W., 1980–1981. Le Carbonifère anté-stéphanien de la Montagne Noire: rapports entre mise en place des nappes et sédimentation. Bulletin B.R.G.M. 2 (I-4), 341–389.

England, P.C., Tompson, A., 1986. Some thermal and tectonic models for crustal melting in continental collision zones. In: Coward, M.P., Ries, A.C. (Eds.). Collision Tectonics. Geological Society of London, Special Publication 19, pp. 83–94.

Faure, M., Cottereau, N., 1988. Données cinématiques sur la mise en place du dôme migmatitique carbonifère moyen de la Zone Axiale de la Montagne Noire (Massif Central, France). Comptes Rendus de l'Académie des Sciences de Paris 307, 1787–1794.

Feist, R., Galtier, J., 1985. Découverte de flores d'âge namurien probable dans le flysch à olistolites de Cabrières (Hérault). Implications sur la durée de la sédimentation synorogénique dans la Montagne Noire (France méridionale). Comptes Rendus de l' Académie des Sciences de Paris 300, 207–212.

Ferret, B., 1983. Les schistes X du Cabardè (versant sud de la Montagne Noire): déformation et métamorphisme. Thesis, University of Toulouse III.

Franke, W., Engel, W., 1986. Synorogenic sedimentation in the Variscan belt of Europe. Bulletin de la Société Géologique de France 8, 25–33.

Gardien, V., Lardeaux, J.M., Ledru, P., Allemand, P., Guillot, S., 1997. Metamorphism during late orogenic extension: insights from the French Variscan belt. Bulletin de la Société Géologique de France 3, 271–286.

Gèze, B., 1949. Etude géologique de la Montagne Noire et des Cévennes méridionales. Mémoire de la Société Géologique de France, Nouvelle Série 29 (62), 1–215.

Graham, R., Hossack, J., Déramond, J., Soula, J.C., 1987. Géométrie des surfaces de chevauchement. Bulletin de la Société Géologique de France 8 (1), 169–181.

Guérangé-Lozes, J., 1987. Les nappes varisques de l'Albigeois cristallin. Lithostratigraphie, volcanisme et déformations. Document B.R.G.M. 135, 259pp.

Guérangé-Lozes, J., Burg, J.P., 1990. Les nappes varisques du sud-ouest du Massif Central (cartes géologiques et structurales à 1/250,000 Montpellier et Aurillac). Géologie de la France 3-4, 71–106.

Hamet, J., Allègre, C.J., 1976. Hercynian orogeny in the Montagne Noire

(France). Application of Rb^{87}–Sr^{87} systematics. Geological Society of America Bulletin 87, 1429–1442.

Hippertt, J.F., 1994. Structures indicative of helicoidal flow in a migmatitic diapir (Baçao complex, southeastern Brazil). Tectonophysics 234, 169–196.

Hippertt, J., Davis, B., 2000. Dome emplacement and formation of kilometre-scale synclines in a granite-greenstone terrain (Quadrilàtero Ferrifero, southeastern Brazil). Precambrian Research 102, 99–121.

Holm, D.K., Lux, D.R., 1996. Core complex model proposed for gneiss dome development during collapse of the Paleoproterozoic Penokean orogen, Minnesota. Geology 24, 343–346.

Holtz, F., Johannes, W., 1994. Maximum and minimum water contents of granitic melts: implications for chemical and physical properties of ascending magmas. Lithos 32, 149–159.

Hudleston, P.J., 1973. Fold morphology and some geometrical implications of theories of fold development. Tectonophysics 16, 1–46.

Kosakowski, G., Kunert, V., Clauser, Ch., Franke, W., Neugebauer, H.J., 1999. Hydrothermal transients in Variscan crust; paleotemperature mapping and hydrothermal models. Tectonophysics 306, 325–344.

Latouche, L., 1968. Contribution à l'étude géologique des Monts de St. Gervais (Hérault). Thesis, University of Orsay.

Laumonier, B., Marignac, Ch., 1996. Les effets respectifs de la compression puis de l'extension tardi-orogéniques hercyniennes dans l'évolution structurale du synclinal de Rosis et de l'anticlinal du Caroux (Est de la Zone Axiale de la Montagne Noire, France). Comptes Rendus de l'Académie des Sciences de Paris 323, 427–434.

Legrand, X., 1990. Effets de la tectonique extensive en milieu continental: le bassin permien de Saint-Affrique. Thesis, University of Toulouse III.

Legrand, X., Soula, J.C., Rolando, J.P., 1991. Effet d'une inversion tectonique négative dans le Sud du Massif Central français: la structure "roll-over" du bassin permien de Saint-Affrique. Comptes Rendus de l'Académie des Sciences de Paris 312, 1021–1026.

Legrand, X., Soula, J.C., Rolando, J.P., 1994. The Saint-Affrique Permian basin (southern France): an example of a roll-over controlled alluvial sedimentation during regional extensional tectonics. Geodynamica Acta 7, 103–120.

Lescuyer, J.L., Cocherie, A., 1992. Datation sur monozircon des métadacites de Sériès: arguments pour un âge protérozoïque terminal des "schistes X" de la Montagne Noire (Massif Central français). Comptes Rendus de l'Académie des Sciences de Paris 314, 1071–1077.

McClay, K.R., 1992a. Thrust Tectonics. Chapman & Hall, London.

McClay, K.R., 1992b. Glossary of thrust tectonics terms. In: McClay, K.R. (Ed.). Thrust Tectonics. Chapman & Hall, London, pp. 419–433.

Maluski, H., Costa, S., Echtler, H., 1991. Late Variscan tectonic evolution by thinning of earlier thickened crust. An ^{40}Ar–^{39}Ar study of the Montagne Noire, southern Massif Central, France. Lithos 26, 287–304.

Marshak, S., Alkmin, F.F., 1989. Proterozoic contraction/extension tectonics of the southern Sao Francisco region, Minas Gerais, Brazil. Tectonics 8, 555–571.

Marshak, S., Tinkham, D., Alkmin, F., Brueckner, H., Bornhorst, T., 1997. Dome-and-keel provinces formed during Paleoproterozoic orogenic collapse-core complexes, diapirs, or neither?: examples from the Quadrilatero Ferrifero and the Penokean orogen. Geology 25 (5), 415–418.

Matte, Ph., 1991. Accretionary history and crustal evolution of the Variscan belt in western Europe. Tectonophysics 196, 309–337.

Matte, Ph., Lancelot, J., Mattauer, M., 1998. La Zone Axiale hercynienne de la Montagne Noire n'est pas un "metamorphic core complex" extensif mais un anticlinal post-nappe à coeur anatectique. Geodinamica Acta 11 (1), 13–22.

Mattauer, M., Laurent, Ph., Matte, P., 1996. Plissement hercynien synschisteux post-nappe et étirement subhorizontal dans le versant sud de la Montagne Noire. Comptes Rendus de l'Académie des Sciences de Paris, 322, 309–315.

Mehnert, K.R., 1968. Migmatites and the Origin of Granitic Rocks. Elsevier Science, New York.

Ménard, G., Molnar, P., 1988. Collapse of a Hercynian Tibetan plateau into a late Paleozoic European basin and range Province. Nature 334, 235–237.

Midgley, J.P., Blundell, D.J., 1997. Deep seismic structure and thermomechanical modelling of continental collision zones. Tectonophysics 273, 155–167.

Odin, G.S., Odin, C., 1990. Echelle numérique des temps géologiques: mise à jour 1990. Géochronique 35, 12–21.

Ourzik, A., 1993. Evolution structuro-métamorphique du dôme de l'Agout sensu lato. Conséquences sur l'évolution géodynamique de la Montagne Noire. Thesis, University of Toulouse III.

Ourzik, A., Debat, P., Mercier, A., 1991. Evolution métamorphique de la partie N et NE de la Zone Axiale de la Montagne Noire (Sud du Massif Central, France). Comptes Rendus de l'Académie des Sciences de Paris 313, 1547–1553.

Palmeri, R., 1997. *P–T* paths and migmatite formation: an example from Deep Freeze Rang, northern Victoria Land, Antarctica. Lithos 42, 47–66.

Paterson, S.R., Miller, R.B., 1998. Mid-crustal magmatic shetts in the Cascades Mountains, Washington: implications for magma ascent. Journal of Structural Geology 20, 1345–1363.

Perchuk, L., Lavrent'eva, I.V., 1983. Experimental investigations of exchange equilibria in the system cordierite–garnet–biotite. In: Saxena, S.K. (Ed.). Kinetics and Equilibrium in Minerals Reactions. New York: Springer-Verlag, pp. 199–240.

Perez-Estáun, A., Martinez-Catalan, J.R., Bastida, F., 1991. Crustal thickening and deformation sequence in the footwall to the suture of the Variscan belt of NW Spain. Tectonophysics 191, 243–253.

Petford, N., 1996. Dykes and diapirs? Transactions of the Royal Society of Edinburgh, Earth Sciences 87, 115–124.

Philippot, P., 1990. Opposite vergence of nappes and crustal extension in the French–Italian Alps. Tectonics 9, 1143–1164.

Ramberg, H., 1967. Gravity Deformation and the Earth's Crust. Academic Press, London (first edition).

Ramberg, H., 1981. Gravity, Deformation and the Earth's Crust. Academic Press, London (second edition).

Ramsay, J.G., 1967. Folding and Fracturing of Rocks. McGraw-Hill, New York.

Reille, J.L., 1978. Mise en évidence des formations hypovolcaniques alcalines cambriennes parmi les orthogneiss hercyniens de la Zone Axiale de la Montagne Noire, d'après l'étude des populations de zircons. Conséquences géologiques. Comptes Rendus de l'Académie des Sciences de Paris, 579–582.

Robie, R.A., Bethke, P.M., Toulmin, M.S., Edwards, J.L., 1966. X-ray crystallographic data, density and molar volumes of minerals. In: Clark Jr., S.P. (Ed.). Handbook of Physical Constants. Memoirs of the Geological Society of America 97, pp. 27–74.

Robin, P.Y., 1979. Theory of metamorphic segregation and related processes. Geochimica and Cosmochimica Acta 43, 1587–1600.

Rolando, J.P., Doubinger, J., Bourges, P., Legrand, X., 1988. Identification de l'Autunien supérieur, du Saxonien et du Thuringien inférieur dans le bassin de Saint-Affrique (Aveyron, France). Corrélations séquentielles et chronostratigraphiques avec les bassins de Lodève, Saint-Affrique et Rodez (Aveyron). Comptes Rendus de l'Académie des Sciences de Paris 307, 14591464.

Roure, F., Polino, R., Nicilich, R., 1990. Early neogene deformation beneath the Po plain: constraints on the post-collisional Alpine evolution. Mémoire de la Société Géologique de France 156, 309–322.

Rushmer, T., 1995. An experimental deformation study of partially molten amphibolite: Application to low-melt fraction segregation. Journal of Geophysical Research 100, 15681–15695.

Rushmer, T., 1996. Melt segregation in the lower crust: how have experiments helped us?. Transactions of the Royal Society of Edinburgh, Earth Sciences 87, 73–83.

Rutter, E.H., Neumann, D.H.K., 1995. Experimental deformation of partially molten Westerly granite under fluid-absent conditions, with implications for the extraction of granitic magmas. Journal of Geophysical Research 100, 15697–15715.

Sawyer, E.W., 1996. Melt segregation and magma flow in migmatites: implications for generation og granite magmas. Transactions of the Royal Society of Edinburgh, Earth Sciences 87, 85–94.

Schuiling, R.D., 1960. Le dôme gneissique de l'Agout (Tarn et Hérault). Mémoire de la Société géologique de France 39, 1–59.

Schuiling, R.D., 1963. Quelques données nouvelles sur la pétrographie du dôme gneissique de l'Agout (Tarn et Hérault). Comptes Rendus sommaires de la Société géologique de France, 219–221.

Schuiling, R.D., De Widt, J., 1962. Sur la genèse du dôme gneissique de l'Agout (Dépts Tarn et Hérault). Geologie en Mijnbouw 41, 321–326.

Schneider, D., Holm, D., Lux, D., 1996. On the origin of Early Proterozoic gneiss domes and metamorphic nodes, northern Michigan. Canadian Journal of Earth Sciences 33, 1053–1063.

Seward, D., Mancktelow, N.S., 1994. Neogene kinematics of the Central and Western Alpes: evidence from fission tracks dating. Geology 2, 803–806.

Shackleton, R.M., 1995. Tectonic evolution of greenstone belts. In: Coward, M.P., Ries, A.C. (Eds.). Early Precambrian Processes. Geological Society London, Special Publication 95, pp. 53–65.

Skinner, B.J., 1966. Thermal expansion. In: Clark Jr, S.P. (Ed.). Hanbook of Physical Constants. Memoirs of the Geological Society of America 97, pp. 75–96.

Snowden, P.A., Bickle, M.J., 1976. The Chindomora Batholith: diapiric intrusion or interference fold? Journal of the Geological Society, London 132, 131.

Soula, J.C., 1969. Evolution structurale de l'Arize orientale. Thesis, University of Toulouse III.

Soula, J.C., 1982. Characteristics and mode of emplacement of gneiss domes and plutonic domes in central-eastern Pyrenees. Journal of Structural Geology 4, 313–342.

Soula, J.C., Debat, P., Déramond, J., Pouget, P., 1986. A dynamical model of the structural evolution of the Hercynian Pyrenees. Tectonophysics 129, 29–51.

Specht, M., Déramond, J., Souquet, P., 1991. Relations tectonique-sédimentation dans les bassins d'avant-pays: utilisation des surfaces stratigraphiques isochrones comme marqueurs de la déformation. Bulletin de la Société Géologique de France 162, 553–562.

Steck, A., Hunziker, J.C., 1994. The Tertiary structural and thermal evolution of the Central Alps. Compressional and extensional structures in an orogenic belt. Tectonophysics 238, 229–254.

Stüwe, K., Barr, T.D., 1998. On uplift and exhumation during convergence. Tectonics 17, 80–88.

Suppe, J., Medwedeff, D.A., 1990. Geometry and kinematics of fault-propagation folding. Eclogae Geologicae 89, 409–454.

Talbot, C.J., Koyi, H., 1995. Paleoproterozoic interplating exposed by resultant gravity overturn near Kiruna, northern Sweden. Precambrian Research 72, 199–225.

Thompson, P.H., Bard, J.P., 1982. Isograds and mineral assemblages in the Eastern Axial Zone, Montagne Noire (France). Implications for temperature gradients and P/T history. Canadian Journal of Earth Sciences 19 (I), 129–143.

Vachard, D., 1974. Contribution à l'étude stratigraphique et micropaléontologique (Algues et Foraminifères) du Dévonien-Carbonifère inférieur de la partie orientale du versant méridional de la Montagne Noire (Hérault, France). Thesis, University of Montpellier.

Van Den Driessche, J., Brun, J.P., 1991–1992. Tectonic evolution of the Montagne Noire (French Massif Central): a model of extensional gneiss dome. Geodinamica Acta 5, 85–99.

Vanderhaeghe, O., 1999. Pervasive melt migration from migmatites to leucogranite in the Shuswap metamorphic core complex, Canada: control of regional deformation. Tectonophysics 312, 35–55.

Van der Molen, I., Paterson, M.S., 1979. Experimental deformation of partially-melted granite. Contribution of Mineralogy and Petrology 70, 299–318.

Vissers, R.L.M., Platt, J.P., Van der Val, D., 1995. Late orogenic extension of the Betic Cordillera and the Alboran domain: a lithospheric view. Tectonics 14 (4), 786–803.

Warren, R.G., Ellis, D.J., 1996. Mantle underplating, granite tectonics, and metamorphic P-T-t paths. Geology 24 (7), 663–666.

Weinberg, R.F., 1996. Ascent mechanism of felsic magmas: news and views. Transactions of the Royal Society of Edinburgh, Earth Sciences 87, 95–103.

Wernicke, B., 1981. Low-angle normal fault in the Basin and Range Province: nappe tectonics in an extending orogen. Nature 291, 645–648.

Wernicke, B., Burchfiel, B.C., 1982. Modes of extensional tectonics. Journal of Structural Geology 4, 105–115.